Suppression of integrin α3β1 by α9β1 in the epidermis controls the paracrine resolution of wound angiogenesis

Whitney M. Longmate,[2] Scott P. Lyons,[2] Sridar V. Chittur,[3] Kevin M. Pumiglia,[2] Livingston Van De Water,[1,2*] and C. Michael DiPersio[1,2*]

[1]Department of Surgery and [2]Department of Regenerative and Cancer Cell Biology, Albany Medical College, Albany, NY 12208
[3]Center for Functional Genomics, University at Albany, Rensselaer, NY 12144

Development of wound therapies is hindered by poor understanding of combinatorial integrin function in the epidermis. In this study, we generated mice with epidermis-specific deletion of α3β1, α9β1, or both integrins as well as keratinocyte lines expressing these integrin combinations. Consistent with proangiogenic roles for α3β1, α3-null keratinocytes showed reduced paracrine stimulation of endothelial cell migration and survival, and wounds of epidermis-specific α3 knockout mice displayed impaired angiogenesis. Interestingly, α9β1 in keratinocytes suppressed α3β1-mediated stimulation of endothelial cells, and wounds of epidermis-specific α9 knockout mice displayed delayed vascular normalization and reduced endothelial apoptosis, indicating that α9β1 cross-suppresses α3β1 proangiogenic functions. Moreover, α9β1 inhibited α3β1 signaling downstream of focal adhesion kinase (FAK) autoactivation at the point of Src-mediated phosphorylation of FAK Y861/Y925. Finally, α9β1 cross-suppressed many α3β1-dependent genes, including the gene that encodes MMP-9, which we implicated as a regulator of integrin-dependent cross talk to endothelial cells. Our findings identify a novel physiological context for combinatorial integrin signaling, laying the foundation for therapeutic strategies that manipulate α9β1 and/or α3β1 during wound healing.

Introduction

During cutaneous wound healing, epidermal keratinocytes contribute to dynamic remodeling of the wound microenvironment by secreting growth factors, cytokines, and proteases that mediate paracrine stimulation of other cells with essential roles in angiogenesis, inflammation, scar formation, and tissue remodeling (Santoro and Gaudino, 2005). Although microenvironmental cues that regulate paracrine signals from the wound epidermis are not yet clear, changes in the ECM are likely to play an important role. Integrins are the major cell surface receptors for the ECM, and their roles in regulating cell adhesion and migration are well known (Hynes, 2002). Importantly, integrins also function as bidirectional signaling receptors that regulate both outside-in signals that control cellular responses to extracellular cues and inside-out signals that control cell-mediated modifications of the microenvironment (Giancotti and Ruoslahti, 1999; Hynes, 2002; Ridley et al., 2003). Different integrins expressed in the epidermis can control numerous keratinocyte functions that are essential for normal wound healing, including reepithelialization, matrix assembly/remodeling, epidermal–dermal adhesion, cell survival, cell proliferation, and paracrine cross talk to the vasculature (Grose et al., 2002; Margadant et al., 2009; Mitchell et al., 2009; Singh et al., 2009; Koivisto et al., 2014; Longmate and DiPersio, 2014; Longmate et al., 2014). Given their roles in controlling both cell-autonomous and paracrine functions, epidermal integrins are attractive therapeutic targets to modulate insufficient healing (e.g., chronic wounds) or exuberant healing (e.g., hypertrophic scars; Koivisto et al., 2014).

Despite recent progress in developing integrins as therapeutic targets for several diseases and pathologies (Goodman and Picard, 2012), the development of integrin-targeting strategies to modulate wound healing has been hindered by our lack of understanding of how different integrins in the epidermis function in combination to effect normal tissue repair and how changes in these integrin interactions may contribute to pathological wound healing. Epidermal keratinocytes express several different integrins with distinct and overlapping roles that collectively contribute to wound healing (Margadant et al., 2010; Koivisto et al., 2014; Longmate and DiPersio, 2014). These

*L. Van De Water and C.M. DiPersio contributed equally to this paper.

Correspondence to C. Michael DiPersio: dipersm@mail.amc.edu

Abbreviations used: cFN, cellular FN; DMBA, 7,12-dimethylbenzanthracine; FN, fibronectin; HUVEC, human umbilical vein endothelial cell; IRES, internal ribosome entry site; MK, mouse keratinocyte; MMP, matrix metalloproteinase; SCC, squamous cell carcinoma; TPA, 12-*O*-tetradecanoylphorbol-13-acetate.

© 2017 Longmate et al. This article is distributed under the terms of an Attribution–Noncommercial–Share Alike–No Mirror Sites license for the first six months after the publication date (see http://www.rupress.org/terms/). After six months it is available under a Creative Commons License (Attribution–Noncommercial–Share Alike 4.0 International license, as described at https://creativecommons.org/licenses/by-nc-sa/4.0/).

The Rockefeller University Press $30.00
J. Cell Biol. Vol. 216 No. 5 1473–1488
https://doi.org/10.1083/jcb.201510042

complex roles are impacted by integrin expression patterns as well as the highly dynamic wound ECM that determines temporal and spatial constraints over ligand availability and integrin activation (Koivisto et al., 2014; Longmate and DiPersio, 2014). Therefore, it is necessary to determine how different integrins are required in combination to achieve temporal control of epidermal functions during wound healing. Indeed, it is clear that the β1 subfamily of integrins is essential for normal epidermal function and wound healing, as mice with epidermis-specific ablation of the β1 subunit display severe epidermal defects that include ECM disorganization and impaired wound reepithelialization (Grose et al., 2002). It is also clear that different β1 integrins have combinatorial and/or compensatory roles in wound healing because genetic deletion of individual α subunits in the epidermis (i.e., ablation of specific αβ heterodimers) causes relatively mild defects in epidermal function or wound healing (Zweers et al., 2007; Margadant et al., 2009; Mitchell et al., 2009; Singh et al., 2009; Koivisto et al., 2014; Longmate et al., 2014) and no single α-null mutation phenocopies the epidermis-specific β1-null mutation (Grose et al., 2002). Collectively, these observations highlight the importance of investigating combined contributions of distinct integrins to wound healing.

To begin to address this question, we focused on α9β1 and α3β1 because their expression is up-regulated in keratinocytes after in vivo wounding (Hertle et al., 1991; Singh et al., 2004). Moreover, at least two components of the provisional wound ECM, laminin-332 (LN-332) and cellular fibronectin (FN [cFN]), are major ligands for α3β1 and α9β1, respectively (Nguyen et al., 2000; Watt, 2002; Singh et al., 2004; Litjens et al., 2006; Høye et al., 2012). Our previous work identified critical roles for keratinocyte α3β1 in neobasement membrane assembly as well as production of paracrine-acting factors that stimulate endothelial cell migration in vitro and wound angiogenesis in vivo (Mitchell et al., 2009; Longmate et al., 2014). Consistently, we also showed that α3β1 regulates the expression of keratinocyte genes with known roles in ECM remodeling or paracrine stimulation of angiogenesis, including matrix metalloproteinase-9 (MMP-9) and members of the mitogen-regulated protein (MRP) family (Iyer et al., 2005; Lamar et al., 2008b; Mitchell et al., 2009, 2010; Missan et al., 2015). However, it remains unknown how proangiogenic α3β1 function is temporally regulated during wound healing. Mice with epidermis-specific deletion of α9 have a distinct phenotype where reduced proliferation of keratinocytes leads to a thinner migrating epidermis during wound closure (Singh et al., 2009). However, other roles for α9β1 in keratinocytes are poorly understood, in large part because α9β1 is rapidly lost when keratinocytes are explanted from the epidermis into culture (Choma et al., 2004; Singh et al., 2009).

To investigate the combinatorial roles of α3β1 and α9β1, we generated a panel of mouse keratinocyte (MK) lines (MK cells) that either lack both of these integrins or express them individually or together. In parallel, we used Cre-Lox recombination to generate a matching panel of conditional integrin knockout mice with epidermis-specific deletion of α3β1, α9β1, or both integrins. These complementary models have allowed us to study for the first time the individual and combined functions of these distinct β1 integrins in keratinocytes both in vitro and in vivo. Our findings reveal a novel role for α9β1 in the cross-suppressive regulation of keratinocyte genes and functions that are dependent on α3β1. Indeed, we show that α9β1 expression in MK cells inhibits the ability of α3β1 to promote paracrine-acting factors that stimulate endothelial cell migration and survival. Importantly, this inhibitory effect of α9β1 is also observed in vivo, where healing wounds in mice lacking epidermal α9β1 but expressing α3β1 display a normal angiogenic response but a delay in vascular normalization coincident with reduced endothelial cell apoptosis. These findings indicate that α9β1 acts as a "brake" on proangiogenic α3β1 functions in a manner that is reminiscent of an integrin cross talk mechanism termed by the Ginsberg group and others as "trans-dominant inhibition" (Díaz-González et al., 1996; Calderwood et al., 2004; Gonzalez et al., 2010; Uotila et al., 2014). Interestingly, epidermal deletion of α9β1 did not enhance α3β1-dependent tumor growth in a skin carcinogenesis model, suggesting that this regulation is absent from skin tumors where there is no vascular regression phase. Moreover, we show that α3β1-mediated paracrine stimulation of endothelial cells occurs through a FAK signaling pathway and that α9β1 exerts trans-dominant inhibition of α3β1 signaling downstream of initial FAK autophosphorylation at the point of Src-mediated phosphorylation of FAK. Finally, comparative microarrays from our panel of MK cells reveal that many α3β1-dependent genes, including some involved in matrix remodeling or induction of angiogenesis, are cross-suppressed by α9β1. These findings identify a novel physiological context for coordinated integrin function within wound keratinocytes, wherein α9β1 promotes blood vessel regression and vascular normalization at later stages of wound healing through suppression of α3β1 proangiogenic functions.

Results

Integrin α9β1 abrogates the ability of integrin α3β1 to promote keratinocyte monolayer migration in vitro

As an in vitro model to investigate integrin cross talk, we generated a panel of MK cell lines that lack or express α3β1 or α9β1 either individually or in combination. We took advantage of an established MK cell line that lacks α3β1 because of an α3-null mutation (MKα3$^-$ cells) and a variant in which α3β1 is restored by stable transfection with human α3 (MKα3$^+$ cells; Iyer et al., 2005). Importantly, MKα3$^+$ cells retain migratory and other properties that reflect keratinocyte activation (Choma et al., 2004, 2007; Manohar et al., 2004), and our group has used these lines to identify α3β1-dependent keratinocyte functions that were confirmed using in vivo models (Mitchell et al., 2009). As is typical of cultured keratinocytes, MK cells lack endogenous α9β1 because of down-regulation of α9 subunit expression (DiPersio et al., 2000; Choma et al., 2004; Singh et al., 2009). Therefore, we restored α9 in MKα3$^+$ or MKα3$^-$ cells by stable transduction with a retrovirus in which human α9 expression is linked to GFP through an internal ribosome entry site (IRES) followed by FACS for GFP to select stable populations. Hereafter, these MK variants will be referred to as MKα3$^-$/α9$^-$, MKα3$^+$/α9$^-$, MKα3$^-$/α9$^+$, or MKα3$^+$/α9$^+$ to reflect their integrin subunit expression. Flow cytometry with a mAb to detect either human α3 or human α9, coupled with analysis of GFP, confirmed appropriate and similar cell surface expression of each integrin in these MK variants (Fig. S1). Importantly, both the α3 and α9 subunits pair only with the β1 subunit, so their surface expression reflects the α3β1 and α9β1 integrin heterodimers, respectively (Hynes, 2002).

Previous work from our group demonstrated that α3-null MK cells are defective in persistent sheet migration, instead

scattering as individual cells in scrape wound assays (Choma et al., 2004). To test coordinate roles for α9β1 and α3β1 in migration, we performed scrape wound assays on an LN-332–rich matrix using our panel of MK variants. Consistent with our previous study (Choma et al., 2004), MK cells that lack both α9β1 and α3β1 showed impaired monolayer migration and scattered into the wound, in contrast with cells that express only α3β1 and migrate as a contiguous sheet (Fig. S2 A; compare MKα3^{-}/α9^{-} with MKα3^{+}/α9^{-}). Expression of α9β1 alone (i.e., in the absence of α3β1) failed to restore a normal migration phenotype, indicating a strict requirement for α3β1 (Fig. S2 A; MKα3^{-}/α9^{+}). Remarkably, reconstitution of α9β1 in cells that express α3β1 inhibited wound closure and induced a scattering phenotype that was similar to that in α3β1-deficient cells (Fig. S2 A; compare MKα3^{+}/α9^{+} with MKα3^{-}/α9^{-} and MKα3^{-}/α9^{+}). These results demonstrate that α9β1 exerts a suppressive effect on α3β1-mediated migration in vitro. Of note, these results did not reflect roles for these integrins in wound reepithelialization in vivo, as no differences were observed in the morphology of the wound epidermis (Fig. S2 B) or in the rate of wound closure between control mice and those that lack either or both integrins in the epidermis (Fig. S2 C). This finding is consistent with previous studies in mice with epidermal deletion of α3β1 or α9β1 (Margadant et al., 2009; Singh et al., 2009) and may reflect compensatory migration roles of other integrins in the wound epidermis (Longmate and DiPersio, 2014).

Integrin α9β1 abrogates the ability of integrin α3β1 to promote secretion by keratinocytes of paracrine-acting factors that stimulate endothelial cells

Earlier work from our group showed that α3β1 promotes secretion of factors by MK cells that stimulate endothelial cell migration, thereby identifying α3β1 as a regulator of paracrine factors from the epidermis that promote a proangiogenic wound environment (Mitchell et al., 2009). However, because keratinocytes lose α9β1 expression in culture, its roles in the paracrine stimulation of endothelial cells have not been explored. To test effects of α9β1 on α3β1-induced endothelial cell migration, we compared the ability of our MK variants to stimulate migration of human umbilical vein endothelial cells (HUVECs). Lower chambers of transwells were charged with medium that was conditioned for 24 h by MKα3^{-}/α9^{-}, MKα3^{+}/α9^{-}, MKα3^{-}/α9^{+}, or MKα3^{+}/α9^{+} cells or with unconditioned medium as a baseline control, and stimulation of endothelial cell migration through the filter was quantified. In the absence of α9β1, MK cells expressing α3β1 showed almost twofold greater induction of HUVEC migration than cells lacking α3β1 (Fig. 1, compare MKα3^{+}/α9^{-} with MKα3^{-}/α9^{-}), as we reported previously (Mitchell et al., 2009). In contrast, MK cells that express α9β1 alone failed to enhance HUVEC migration, indicating a strict requirement for α3β1 (Fig. 1, MKα3^{-}/α9^{+}). Remarkably, restoring α9 expression in α3-expressing MK cells suppressed the α3β1-dependent HUVEC migration response (Fig. 1, compare MKα3^{+}/α9^{+} with both MKα3^{-}/α9^{-} and MKα3^{-}/α9^{+}), indicating that α9β1 potently inhibits the ability of α3β1 to induce soluble factors that promote endothelial cell migration.

We next assessed paracrine effects on endothelial cell survival. HUVECs were serum starved to prime them for apoptosis and then treated with conditioned medium from each of the MK variants and compared for either cleaved caspase 3 by immunofluorescence (Fig. 2 A) or levels of caspase 3 activity

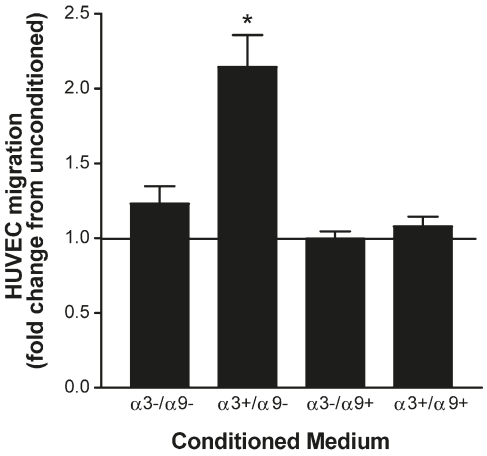

Figure 1. **α9β1 inhibits α3β1-dependent secretion of keratinocyte factors that induce endothelial cell migration.** Transwell assays were performed to compare migration of HUVECs in response to conditioned medium from MK cells that expressed α3β1 and/or α9β1 in various combinations, as indicated. Graph shows HUVEC migration as a fold increase over that in cells treated with unconditioned medium as a baseline (set to 1.0). Means ± SEM are shown. *n* = 3 independent experiments. A one-way analysis of variance with Newman-Keuls's multiple comparisons test was used. *, P < 0.05 compared with nonasterisked groups.

by EnzChek assay (Fig. 2 B). HUVECs treated with conditioned medium from MK cells that express only α3β1 showed a reduction in both apoptotic cell number and caspase 3 activity compared with HUVECs treated with conditioned medium from MK cells that lack α3β1 (Fig. 2, A and B; MKα3^{+}/α9^{-} vs. MKα3^{-}/α9^{-}), indicating a paracrine prosurvival effect of α3β1. Importantly, reconstitution of α9β1 in α3β1-expressing MK cells enhanced HUVEC apoptosis (Fig. 2, A and B; MKα3^{+}/α9^{+} vs. MKα3^{+}/α9^{-}), indicating that α9β1 suppresses the prosurvival effect of α3β1. Collectively, results in Figs. 1 and 2 demonstrate that α9β1 cross-suppresses α3β1-mediated paracrine signaling from keratinocytes that stimulates proangiogenic functions of endothelial cells.

Vascular normalization is impaired in wounds of epidermis-specific α9 knockout mice

To determine whether the suppressive effect of α9β1 over α3β1 that we observed in MK cells reflects a similar role in vivo, we established a panel of mutant mice that express α3β1 alone, α9β1 alone, both integrins, or neither integrin in the epidermis. To generate this panel, mice homozygous for floxed alleles of α3 (Itga3$^{flx/flx}$; Mitchell et al., 2009) or α9 (Itga9$^{flx/flx}$; Singh et al., 2009), either individually or in combination, were crossed with a transgenic line expressing Cre recombinase under control of the keratin 14 promoter (K14-Cre) to restrict integrin deletion to basal keratinocytes of the interfollicular and follicular epidermis. Hereafter, K14-Cre:Itga3$^{flx/flx}$ mice are referred to as α3eKO, K14-Cre:Itga9$^{flx/flx}$ as α9eKO, and K14-Cre:Itga3$^{flx/flx}$:Itga9$^{flx/flx}$ as α3/α9eKO. Littermates lacking K14-Cre served as control mice that express both integrins. α3eKO and α9eKO mice are viable and show efficient deletion of α3β1 or α9β1, respectively, in the epidermis (Mitchell et al., 2009; Singh et al., 2009), and expression of either α3β1 or α9β1 persists in the epidermis when the other is deleted (Fig. S3). Double-knockout α3/α9eKO mice are also viable.

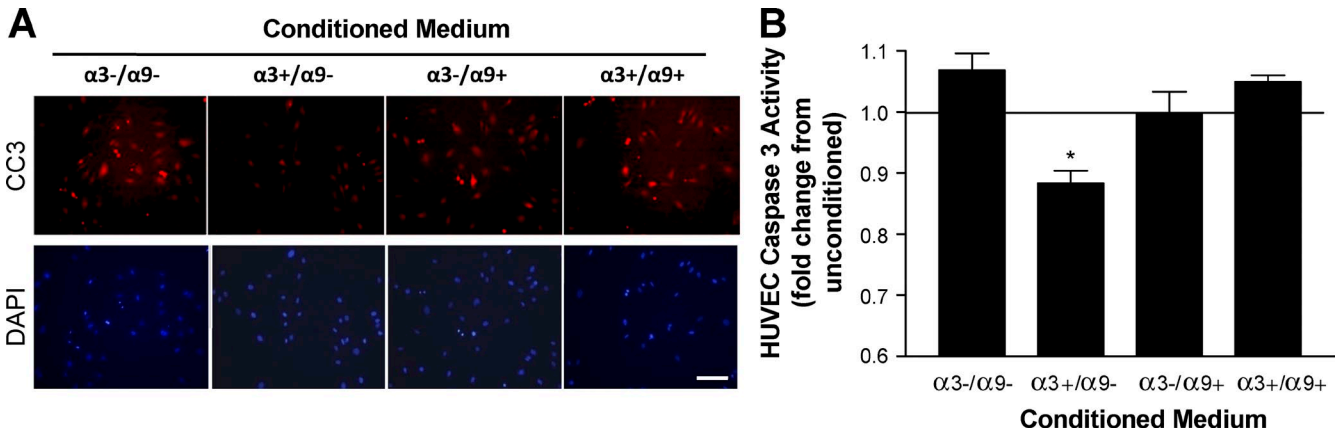

Figure 2. **α9β1 inhibits the α3β1-dependent secretion of keratinocyte factors that suppress endothelial cell apoptosis.** (A and B) HUVEC apoptosis was measured in response to conditioned media from MK cells that express α3β1 and/or α9β1 in various combinations as indicated. (A, top) Apoptotic cells were detected by immunostaining with an antibody against cleaved caspase 3 (CC3). Bottom, DAPI staining of nuclei. Bar, 100 µm. (B) Graph showing relative caspase 3 activity in HUVECs (EnzChek assay) normalized to the daily mean to account for variability by day. Means ± SEM are shown. *n* = 3 independent experiments. A one-way analysis of variance with Newman-Keuls's multiple comparisons test was used. *, P < 0.05 compared with nonasterisked groups.

To assess the effects of epidermal α3 and/or α9 deletion on wound angiogenesis in vivo, we generated 4-mm excisional wounds in our panel of integrin knockout mice and then performed anti-CD31 immunostaining to compare blood vessel density 5 or 10 d after wounding. In this model, wounds of control mice display a robust angiogenic response in 5-d fully reepithelialized wounds (Fig. 3 A, top; Mitchell et al., 2009). Regression of blood vessel density is observed by 10 d after wounding in control mice (Fig. 3 A, bottom). As we previously observed in this model, CD31 staining was reduced in 5-d wounds of α3eKO mice compared with control mice, reflective of a dampened angiogenic response (Fig. 3, A [top] and C; Mitchell et al., 2009). In contrast, vessel density was comparable in 5-d wounds of control and α9eKO mice (Fig. 3, A [top] and C), indicating that the absence of α9β1 does not alter the initial angiogenic response. However, vessel density remained markedly higher in 10-d wounds of α9eKO mice compared with control mice, indicating that vascular normalization was impaired (Fig. 3, A [bottom] and D) and consistent with release of a brake on proangiogenic functions of α3β1. In support of this hypothesis, blood vessel density was reduced in α3/α9eKO mice throughout wound healing (Fig. 3, A, C and D), showing that epidermal α3β1 is required for the persistently high vessel density that occurs in the absence of α9β1. Of note, there were no differences in basal vessel density of unwounded skin from all four genotypes (Fig. 3 B). Collectively, these observations support a model wherein epidermal α3β1 promotes initial wound angiogenesis, whereas α9β1 exerts suppression over α3β1 in a temporally restricted manner, leading to normalized vascular density during the resolution phase of wound healing.

During normal wound healing, the resolution of angiogenesis is accomplished largely through endothelial apoptosis (Wietecha et al., 2013). Consistently, the persistently high vascular density that we observed in 10-d wounds of α9eKO mice was coincident with reduced apoptosis in the wound bed (Fig. 4, A and B). We observed that reduced staining for cleaved caspase 3 frequently colocalized with anti-CD31 staining or occurred adjacent to faded CD31 staining, consistent with apoptosis of endothelial cells (Fig. 4 C, arrows and arrowheads, respectively). These results show that epidermal α9β1 suppresses α3β1-mediated paracrine regulation of vascular survival in vivo, presumably reflecting the suppressive effect of α9β1 on α3β1-mediated endothelial cell survival that we observed in vitro (Fig. 2). Importantly, flow analysis and immunohistochemistry showed that the low levels of endogenous α2β1 and α5β1 and the high levels of endogenous α6 integrins were not altered substantially among our panel of MK cells or mice, respectively, indicating that compensatory changes in expression of other β1 integrins do not occur upon deletion of either α3β1 or α9β1 (Fig. S4).

Genetic deletion of epidermal α9β1 does not enhance α3β1-dependent skin tumor formation

Compelling functional similarities exist between wound keratinocytes and skin tumor cells, such as enhanced migration, proliferation, and production of proangiogenic factors. Expression of α3β1 and α9β1 persists in squamous cell carcinoma (SCC; Häkkinen et al., 1999; Janes and Watt, 2006). Epidermal deletion of α3β1 led to reduced incidence and size of skin papillomas (i.e., benign SCC precursors) that form in response to the 7,12-dimethylbenzanthracine (DMBA)/12-*O*-tetradecanoylphorbol-13-acetate (TPA) two-step carcinogenesis protocol (Sachs et al., 2012). Because α9β1 was required for blood vessel regression during later stages of wound healing (Figs. 3 and 4), we tested whether or not α9β1 has a cross-suppressive effect on α3β1-dependent tumor growth and angiogenesis, in which there is no regression phase. As expected, we observed that neither α3eKO nor α3/α9eKO mice formed papillomas in response to DMBA/TPA treatment compared with control mice, which formed tumors (Fig. 5, A, C, and D), confirming that α3β1 is essential for tumorigenesis (Sachs et al., 2012). Of note, α3β1-dependent tumor incidence was lower in the mixed genetic background of our model compared with that reported by Sachs et al. (2012). We exploited this reduced level of tumorigenesis to assess whether or not epidermal deletion of α9β1 enhances DMBA/TPA-induced papilloma formation above these levels. We observed that tumors in α9eKO mice were fewer and smaller than tumors in control mice that express both integrins, although these trends did not reach statistical significance

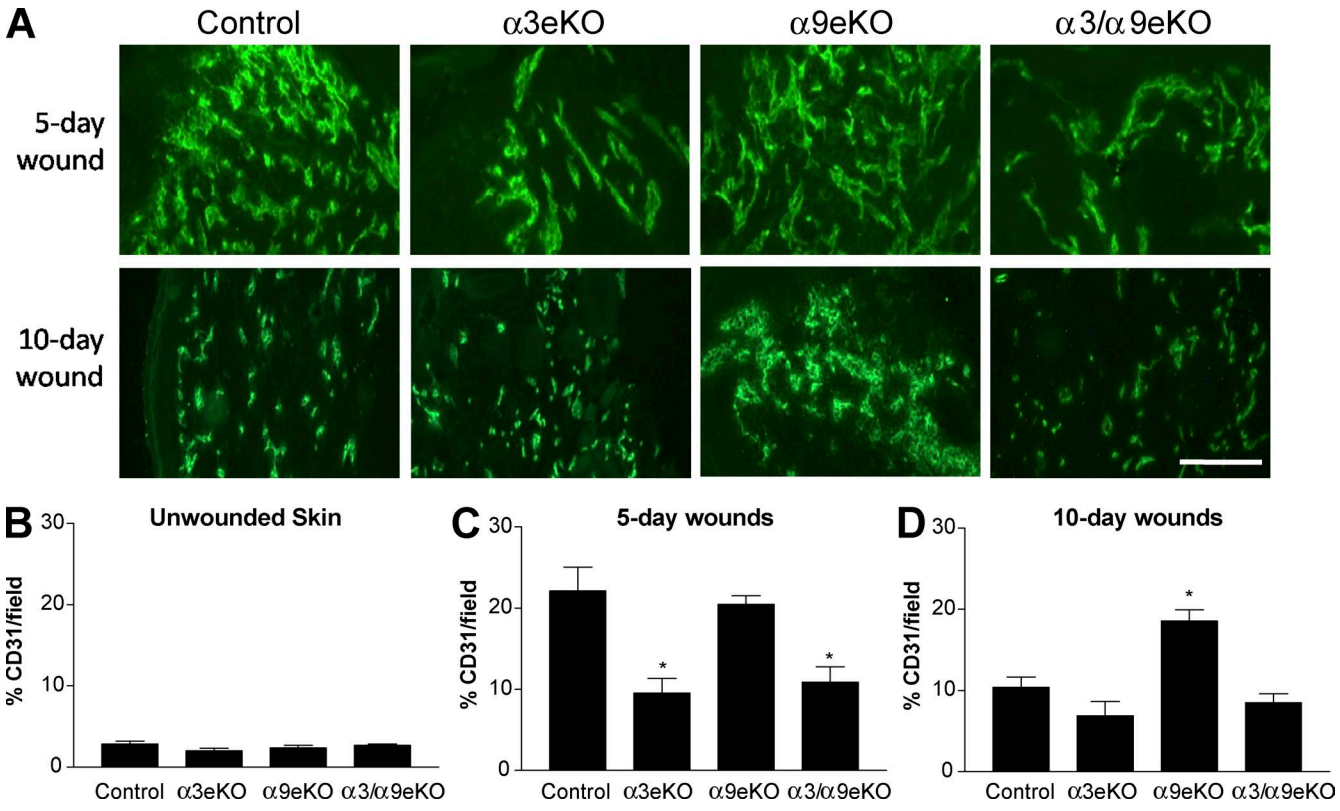

Figure 3. **Resolution of wound angiogenesis is delayed in mice lacking α9β1 in the epidermis.** (A) CD31 immunostaining of cryosections from 5- and 10-d wounds in control, α3eKO, α9eKO, or α3/α9eKO mice. Bar, 100 µm. (B–D) Vessel densities were quantified for each genotype as percentages of CD31-positive staining per field within unwounded skin (B), a 5-d wound bed (C), and a 10-d wound bed (D). Means ± SEM are shown. $n \geq 5$ mice per genotype. A one-way analysis of variance with Newman-Keuls's multiple comparisons test was used. *, $P < 0.05$ compared with nonasterisked groups.

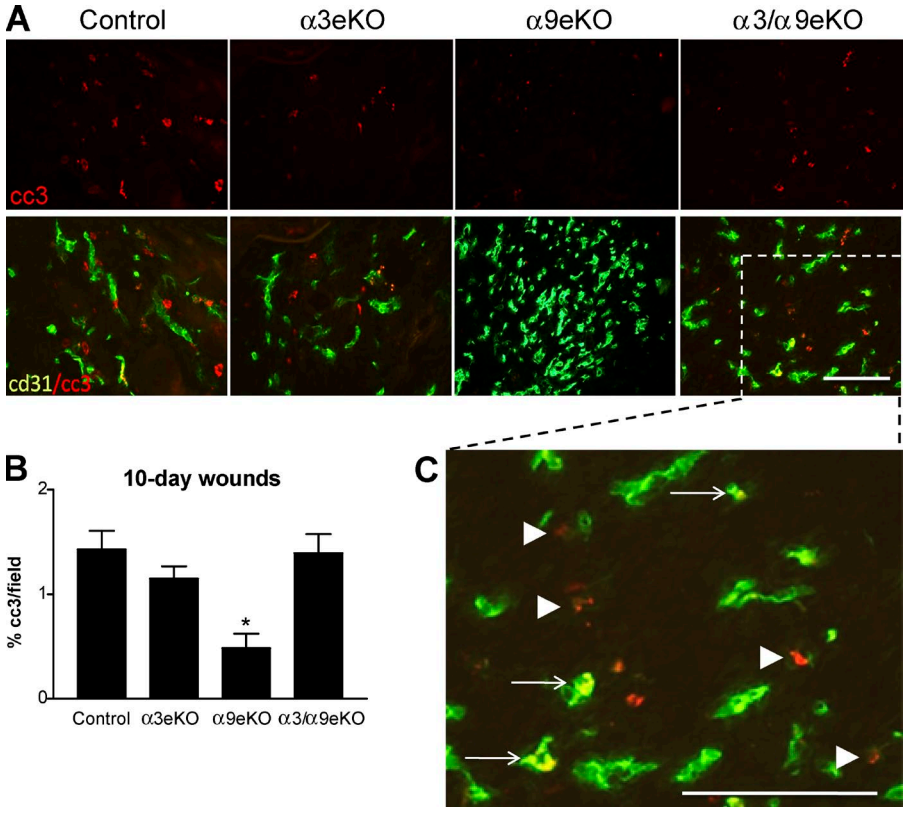

Figure 4. **Persistent vasculature in wounds of α9eKO mice is correlated with a reduced number of apoptotic cells in the wound bed.** (A) Immunostaining for cleaved caspase 3 (cc3; red) and endothelial cell marker CD31 (green) on cryosections from 10-d wounds of control, α3eKO, α9eKO, and α3/α9eKO mice. Top, cleaved caspase 3 alone; bottom, overlay of cleaved caspase 3 with CD31. (B) Cleaved caspase 3 staining was quantified as the percentage of positive staining per field of 10-d wound beds from control, α3eKO, α9eKO, or α3/α9eKO mice. Means ± SEM are shown. $n \geq 5$ mice per genotype. A one-way analysis of variance with Newman-Keuls's multiple comparisons test was used. *, $P < 0.05$ compared with nonasterisked groups. (C) Enlargement of the indicated area from an α3/α9eKO section shows cells with cleaved caspase 3 and CD31 costaining (yellow; arrows) or with cleaved caspase 3 staining (red) adjacent to lighter CD31 staining (faded green; arrowheads), indicating apoptotic endothelial cells. Bars, 100 µm.

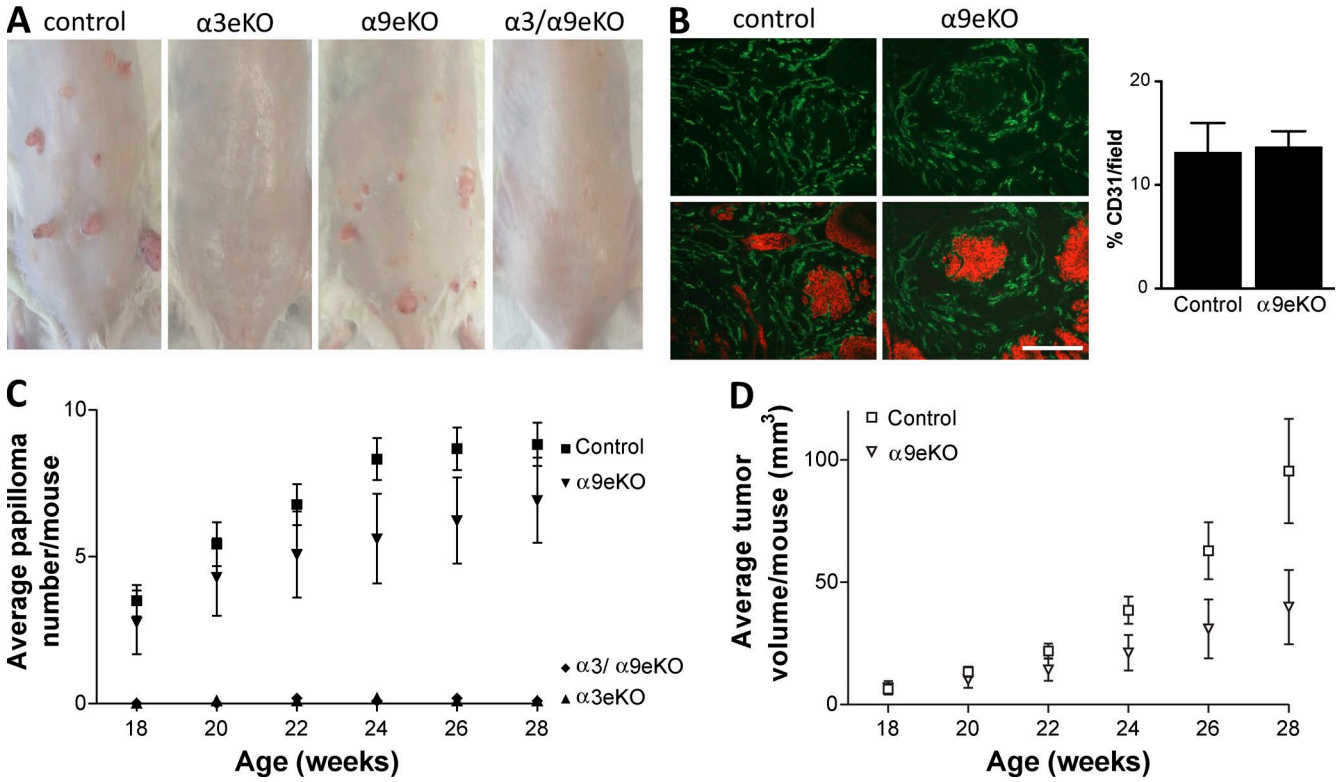

Figure 5. **Epidermal deletion of α9β1 does not alter α3β1-dependent tumorigenesis.** Mice of the indicated genotypes were subjected to the two-step skin carcinogenesis protocol. (A) Images show back skin from a representative mouse of each genotype. (B) Cryosections of papillomas from control or α9eKO mice were immunostained with anti-CD31 (top; green). Bottom panels are merged with anti–keratin 14 to show groups of tumor cells and adjacent stroma. Vessel density is quantified in the graph to the right. $n \geq 5$ tumors per genotype. Bar, 100 µm. (C) Average papilloma number per mouse for each genotype. (D) Average tumor volume per mouse for control and α9eKO. Means ± SEM are shown. $n \geq 11$ mice per genotype. Data from mice of 28 wk of age were subjected to one-way analyses of variance with Newman-Keuls's multiple comparisons (C) or two-tailed *t* tests (D). Tumors from α3eKO and α3/α9eKO mice were significantly fewer and smaller compared with tumors from control mice ($P < 0.05$). Although tumors from α9eKO mice trended toward being fewer and smaller than in control mice, this difference was not statistically significant ($P > 0.05$).

(Fig. 5, A, C, and D). Thus, α9β1 was not only dispensable, but its absence did not enhance α3β1-dependent tumor formation. Furthermore, we did not observe a difference in blood vessel density between papillomas of control and α9eKO mice (Fig. 5 B). These results indicate that the suppression that α9β1 exerts over proangiogenic functions of α3β1 during the regression phase of wound healing does not occur in a tumor setting where angiogenesis persists.

Integrin α9β1 abrogates α3β1-dependent FAK/Src signaling at a point downstream of initial FAK autophosphorylation

Activation of FAK/Src signaling has been linked to integrin-dependent processes in keratinocytes and other epithelial cells (Sieg et al., 2000; Mitra and Schlaepfer, 2006). Integrin α3β1 promotes FAK/Src signaling in keratinocytes, which we have linked to formation of polarized lamellipodia, cell migration, and survival (Manohar et al., 2004; Choma et al., 2007). Given that α9β1 cross-suppressed several α3β1-mediated keratinocyte functions, we wanted to determine whether α9β1 has a cross-suppressive effect on α3β1-dependent activation of FAK. To compare initial FAK activation, cell lysates were immunoblotted for FAK autophosphorylation at Y397. MK cells that lack both α9β1 and α3β1 showed impaired FAK activation compared with cells that express only α3β1 (Fig. 6 A, compare lane 1 with lane 2), confirming α3β1-dependent FAK activation (Choma et al., 2004). Interestingly, enhanced phosphorylation of FAK Y397 was also observed in the presence of both α9β1 and α3β1 (Fig. 6 A, compare lane 1 with lane 4). Moreover, expression of α9β1 was sufficient to induce phosphorylation of FAK Y397 in the absence of α3β1 (Fig. 6 A, compare lane 1 with lane 3). These results indicate that α9β1 promotes FAK autoactivation and does not impair α3β1-mediated FAK activation.

Certain Src family kinases bind to phospho-Y397 of FAK via their SH2 domains, leading to subsequent phosphorylation of FAK residues Y861 and Y925 and creating binding sites for other signaling or adapter proteins that propagate FAK/Src signaling (Cary and Guan, 1999; Schlaepfer and Mitra, 2004). Expression of α3β1 alone in MK cells stimulated FAK phosphorylation at Y861 and Y925 (Fig. 6, B and C; compare lane 1 with lane 2), as we observed previously (Choma et al., 2004). Remarkably, however, expression of α9β1 abrogated α3β1-mediated phosphorylation of both Y861 (Fig. 6 B, compare lane 2 with 4) and Y925 (Fig. 6 C, compare lane 2 with lane 4). Moreover, expression of α9β1 did not itself induce phosphorylation of Y861 or Y925 significantly above background levels (Fig. 6, B and C, compare lane 1 with lane 3). These results indicate that α9β1 abrogates α3β1-mediated FAK/Src signaling at a point downstream of initial FAK autoactivation.

Src-mediated phosphorylation of Y861 and Y925 on FAK creates binding sites for other signaling and adapter proteins,

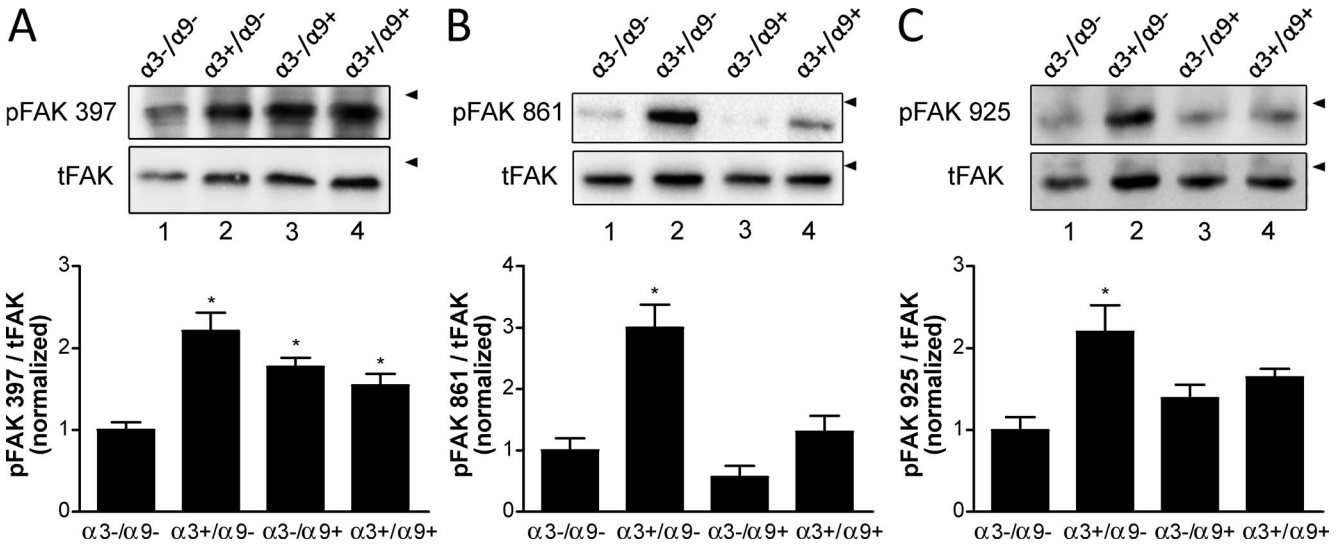

Figure 6. **Expression of α9β1 abrogates α3β1-dependent FAK phosphorylation in MK cells.** (A–C) Cell lysates were assayed by immunoblot for phosphorylation of FAK (pFAK) at tyrosine residues Y397 (A), Y861 (B), and Y925 (C) or total FAK (tFAK). Arrowheads indicate positions of 130-kD markers. Graphs show quantification of phospho-FAK normalized to total FAK from at least three independent experiments. Means ± SEM are shown. $n \geq 3$. One-way analyses of variance with Newman-Keuls's multiple comparisons test were used. *, $P < 0.05$ compared with nonasterisked groups.

including paxillin, thereby linking the FAK/Src signaling complex to downstream effectors such as the Rho family GTPase, Rac, and MAPKs (Cary and Guan, 1999; Schlaepfer and Mitra, 2004). The integrin α9 subunit, like the evolutionarily related α4 subunit, can bind paxillin directly via its cytoplasmic tail (Liu et al., 2001; Young et al., 2001), and paxillin binding to the α tail of α4β1 leads to blunted Rac activation (Nishiya et al., 2005). Thus, it seemed possible that α9β1 may abrogate FAK/Src signaling by titrating paxillin away from an α3β1 complex. To test whether the paxillin-binding site on α9β1 was required for suppression of α3β1-mediated FAK phosphorylation, we transduced MKα3$^+$/α9$^-$ cells with a retrovirus that expresses α9^{W999A}, a previously described mutant of human α9 that fails to bind paxillin (Liu et al., 2001; Young et al., 2001). Flow cytometry confirmed that mutant α9 was expressed in MKα3$^+$/α9^{W999A} cells at a level comparable to that of wild-type α9 in MKα3$^+$/α9$^+$ cells (Fig. S5 A). However, we detected no differences in FAK phosphorylation at Y397, Y861, or Y925 between MKα3$^+$/α9^{W999A} cells and MKα3$^+$/α9$^+$ cells (Fig. S5 B). Moreover, HUVEC migration was comparable in response to conditioned medium from MKα3$^+$/α9^{W999A} cells or MKα3$^+$/α9$^+$ cells (Fig. S5 C). Collectively, these results suggest that the ability of α9β1 to cross-suppress α3β1 does not require the paxillin-binding site on α9.

Inhibiting the ligand-binding function of α9β1 abrogates the cross-suppression of α3β1

Our finding that early proangiogenic functions guided by α3β1 are tempered by α9β1 later in wound healing (Fig. 3) suggests that the ability of α9β1 to modulate α3β1 function is temporally restricted in vivo, perhaps to effect timely normalization of the vasculature during the resolution phase. Because α3β1 and α9β1 are both up-regulated at the onset of wound healing (Hertle et al., 1991; Singh et al., 2004), their temporally coordinated functions might be achieved through binding to ECM ligands that appear at specific stages of wound healing. In support of the latter idea, LN-332 (a major ligand of integrin α3β1) has been shown to be up-regulated immediately upon wounding (Nguyen et al., 2000), whereas cFN (a major ligand of α9β1) is maximally up-regulated at a later stage (~7 d after wounding in the punch biopsy model used here; Singh et al., 2004). Consistently, LN-332 was readily detected 5 d after wounding in our model, whereas cFN levels were low at 5 d but increased considerably at 10 d (Fig. 7 A).

To directly test whether blocking ligand binding by α9β1 abrogates its ability to suppress α3β1-mediated FAK signaling, we treated MKα3$^+$/α9$^+$ cells with the mAb Y9A2 to block α9β1-mediated adhesion, as we described previously (Fig. 7 B; Shinde et al., 2008). Although treatment with Y9A2 did not alter FAK autophosphorylation on residue Y397 (Fig. 7 C), it was able to enhance phosphorylation of FAK Y925 in MKα3$^+$/α9$^+$ cells (Fig. 7 D). Moreover, pretreatment of MKα3$^+$/α9$^+$ cells with Y9A2 enhanced paracrine stimulation of endothelial cell migration (Fig. 7 E). These results indicate that ECM ligand binding controls the ability of α9β1 to suppress α3β1.

Integrin α9β1 cross-suppresses α3β1-dependent gene expression in keratinocytes

Our group previously reported that α3β1-deficient MK cells produce markedly less of two secreted proangiogenic factors, MMP-9 and MRP-3 (Iyer et al., 2005; Mitchell et al., 2009). Moreover, we determined that deletion of α3 from MK cells leads to altered expression of other genes with known roles in angiogenesis or other aspects of tissue remodeling (Missan et al., 2014). To determine the extent to which α9β1 modulates α3β1-dependent genes, we performed microarray analysis to examine the transcriptomes of MK cells that express only α3β1 (MKα3$^+$/α9$^-$), only α9β1 (MKα3$^-$/α9$^+$), or both integrins (MKα3$^+$/α9$^+$), each compared with baseline gene expression in MK cells lacking both integrins (MKα3$^-$/α9$^-$). We identified a cohort of 176 genes with regulatory patterns that indicate α9β1 cross-suppression of α3β1 (i.e., an α3β1-dependent change in expression was reversed to baseline levels by the presence of α9β1; Fig. 8, A and B). Fig. 8 C lists a small subset of genes that fit this regulatory pattern according to the following criteria: (a) expression was increased or decreased by more than twofold

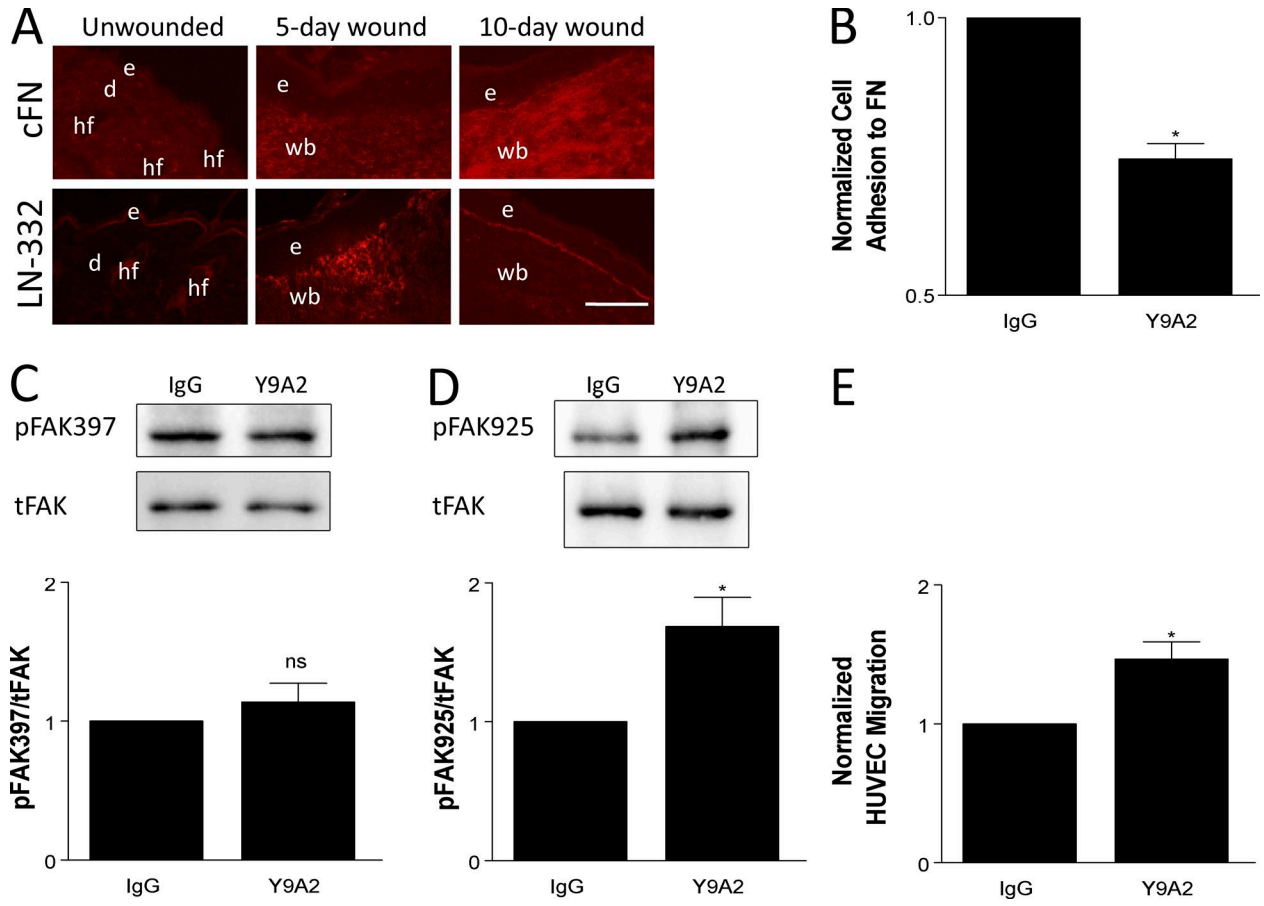

Figure 7. **Inhibiting the ligand-binding function of α9β1 abrogates cross-suppression of α3β1.** (A) Immunostaining for cFN (top) or LN-332 (bottom) on cryosections from unwounded skin, 5-d wounds, and 10-d wounds of control mice. LN-332 is up-regulated by 5 d after wounding, whereas cFN is most abundant in 10-d wounds. $n \geq 4$ mice per time point. Bar, 100 µm. d, dermis; e, epidermis; hf, hair follicle; wb, wound bed. (B–E) MK cells were treated with 10 µg/ml Y9A2 (α9β1 function-blocking antibody) or mouse IgG as control. (B) Treated MKα3$^-$/α9$^+$ cells were analyzed in adhesion assays to validate that Y9A2 reduced α9β1 binding to cFN. (C and D) Cell lysates from treated MKα3$^+$/α9$^+$ cells were assayed by immunoblot for FAK phosphorylation at tyrosine residues Y397 (C) and Y925 (D), as indicated. Graphs show quantitations from three independent experiments. tFAK, total FAK. (E) Transwell assays were performed as in Fig. 1 to compare the HUVEC migration response to conditioned media from treated MKα3$^+$/α9$^+$ cells. Data are normalized to the IgG control. Means ± SEM are shown. $n \geq 3$ independent experiments. A Student's *t* test was used. *, $P < 0.05$; ns, not significant.

in response to α3β1 alone (column A), (b) expression was restored to near-baseline levels (<1.5-fold difference) when α9β1 was introduced into α3β1-expressing cells (column B), and (c) there was little or no change in baseline expression when α9β1 was expressed alone (column C). This pattern reveals α3β1-dependent gene regulation that is subject to suppression by α9β1, where α9β1 has little or no independent effect (i.e., the opposing effects of α9β1 are not because of a simple balancing effect). We also observed other gene regulatory patterns, including elevation or depression by α3β1 or α9β1 alone and cooperative elevation or depression by α3β1 and α9β1. The full microarray dataset is available at the Gene Expression Omnibus (series accession no. GSE73826).

Interestingly, α9β1 suppressed several α3β1-dependent genes that encode secreted proteins involved in angiogenesis and/or ECM remodeling, including several MMPs (Fig. 8, B and C). Although MMP-9 was not detected on our array, we determined that α3β1-dependent expression of MMP-9, described previously (DiPersio et al., 2000; Iyer et al., 2005), was also cross-inhibited by α9β1. Indeed, MMP-9 was α3β1 dependent at the levels of both mRNA (quantitative PCR; Fig. 8 D) and secreted protein (gelatin zymography; Fig. 8 E). Moreover, MMP-9 was significantly reduced in cells that expressed both α9β1 and α3β1 (i.e., MKα3$^+$/α9$^+$) compared with cells that express α3β1 alone (i.e., MKα3$^+$/α9$^-$), whereas α9β1 alone had no independent effect on MMP-9 expression (Fig. 8, D and E).

Perturbation of FAK phosphorylation at Y861 or Y925 in α3β1-expressing keratinocytes reduces MMP-9 secretion and cross talk to endothelial cells

Results in Fig. 6 indicate that the α9β1-mediated cross-suppression of α3β1 signaling occurs downstream of initial FAK activation and that the point of convergence is upstream of Src-mediated phosphorylation of FAK at Y861 and Y925. To determine the importance of these sites for α3β1-dependent cross talk to endothelial cells, we infected MKα3$^+$/α9$^-$ cells (i.e., lacking α9β1) with adenoviruses that encode GFP-tagged FAK mutants, FAK:Y861F or FAK:Y925F, each of which is mutated at the respective tyrosine and functions as a dominant-negative suppressor of endogenous FAK (Fig. 9 A). As a control, cells were infected with adenovirus encoding GFP-tagged wild-type FAK (FAK:WT; Fig. 9 A). HUVEC migration toward conditioned medium from MK cells infected with either FAK

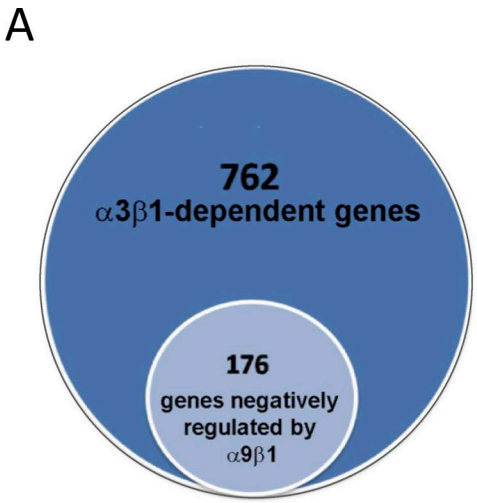

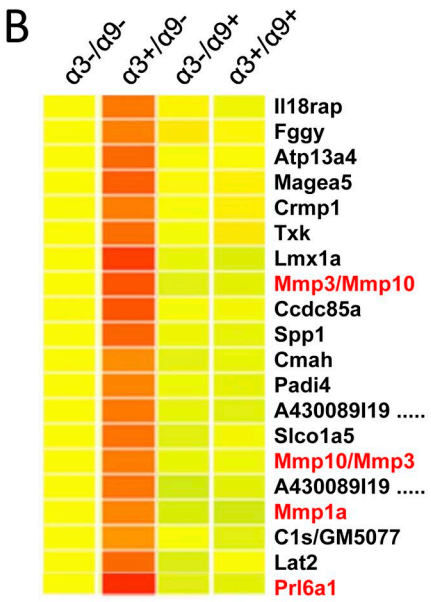

C

Gene Symbol	Gene Description	Fold-change over baseline in MKα3-/α9-; avg., n=2		
		A MKα3+/α9-	B MKα3+/α9+	C MKα3-/α9+
Examples of genes where α3β1-dependent increase is suppressed by α9β1:				
Stfa1	Stefin A1	20.52	1.43	1.18
Stfa3	Stefin A3	11.41	-1.13	-1.03
Prl6a1	prolactin family 6, subfamily a, member 1	8.94	-1.25	-1.23
Prl3d1	prolactin family 3, subfamily d, member 1	2.29	-1.15	-1.17
Prl2a1	prolactin family 2, subfamily a, member 1	2.15	-1.10	1.18
Mmp3	matrix metalloproteinase 3 (MMP-3)	5.70	-1.38	-1.40
Mmp10	matrix metalloproteinase 10 (MMP-10)	3.76	-1.14	-1.24
Prss22	serine protease 22	2.08	1.22	-1.07
Examples of genes where α3β1-dependent decrease is suppressed by α9β1:				
Celsr2	cadherin, EGF LAG seven-pass G-type receptor 2	-2.15	-1.35	1.36
Fgfr2	fibroblast growth factor receptor 2	-4.98	1.01	2.31

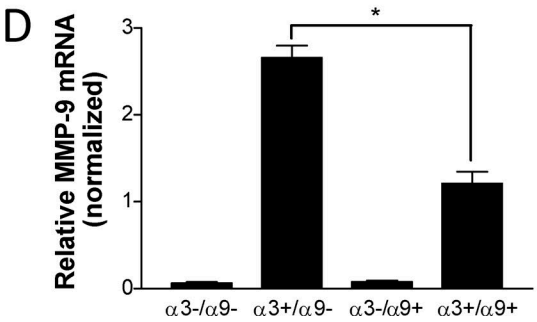

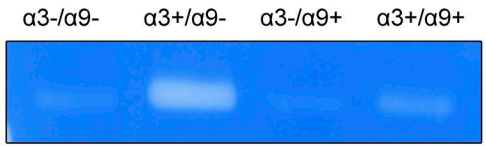

Figure 8. **Integrin α9β1 reverses a subset of α3β1-dependent changes in gene expression in MK cells.** (A–C) Whole-genome transcriptome was compared between MK cell variants that express α3β1 and α9β1 in various combinations. The complete gene list was submitted to the Gene Expression Omnibus (series accession no. GSE73826). (A) Venn diagram showing that 23% of α3β1-dependent genes were restored to baseline expression by coexpression of α9. (B and C) Heat map and microarray data for a subset of gene array results indicate a pattern of cross-suppressive regulation of α3β1 by α9β1. (B) Heat map: genes for matrix metalloproteins or MRPs/proliferins are in red text. (C) Abbreviated list of genes implicated in epidermal biology, ECM remodeling, and/or angiogenesis. LAG, laminin G. (D) MMP-9 mRNA expression was determined for the MK cell variants by quantitative PCR. Data were normalized to β-actin mRNA. Means ± SEM are shown. $n = 3$ independent experiments. A one-way analysis of variance with Newman-Keuls's multiple comparisons test was used. *, $P < 0.05$. (E) Gelatin zymography for secreted MMP-9 was performed using conditioned medium generated from MK cells. A representative zymograph from three independent experiments is shown.

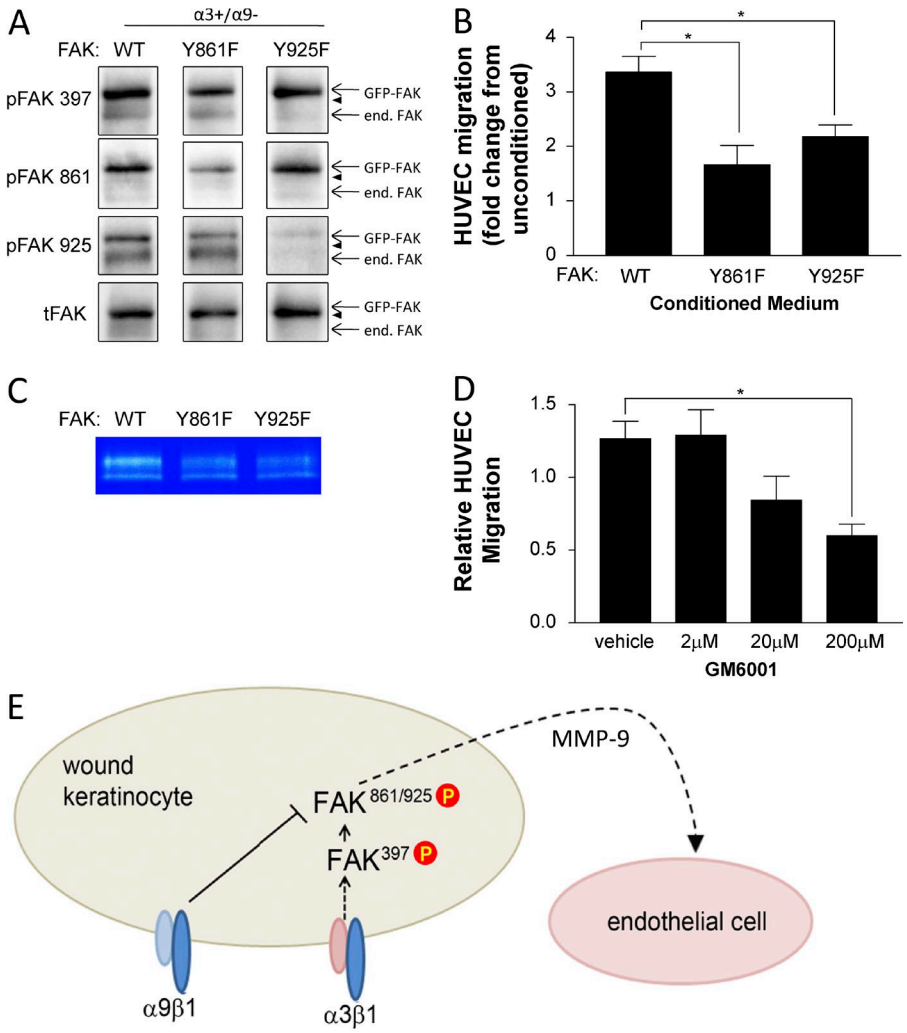

Figure 9. **Perturbation of FAK phosphorylation at Y861 or Y925 in α3β1-expressing keratinocytes reduces MMP-9 secretion and cross talk to endothelial cells.** (A and B) MK $\alpha3^+/\alpha9^-$ cells were infected for 24 h with adenovirus expressing GFP-tagged FAK:WT, FAK:Y861F, or FAK:Y925F and then grown to confluence on collagen. Cells were lysed to assess expression and phosphorylation of GFP-FAK fusion proteins (A), or conditioned medium was harvested and HUVEC migration response was assessed as in Fig. 1 (B). (A) Representative immunoblots confirm comparable expression of GFP-FAK variants and appropriately reduced phosphorylation of the mutated tyrosine. Arrowheads indicate positions of 130-kD markers. end. FAK, endogenous FAK; tFAK, total FAK. (B) Graph shows HUVEC migration in response to conditioned medium from GFP-FAK–infected MK cells relative to unconditioned media as a baseline (set to 1.0). (C) Secreted MMP-9 was assessed by gelatin zymography of MK-conditioned medium from $\alpha3^+/\alpha9^-$ cells infected with wild type (WT) or mutant FAK adenoviruses. A representative zymograph from three independent experiments is shown. (D) Conditioned medium from MK$\alpha3^+/\alpha9^-$ cells was treated with the MMP inhibitor GM6001, and the HUVEC migration response was assessed. Means ± SEM are shown. *n* = 3 independent experiments. One-way analyses of variance followed by Dunnett's multiple comparisons test were used. *, $P \leq 0.05$. (E) Model showing how α9β1 exerts its suppressive effect on α3β1 signaling downstream of FAK autoactivation at the point of Src-mediated phosphorylation of FAK Y861/Y925, leading to reduced cross talk to the endothelium partly through reduced secretion of MMP-9. P, phosphorylation.

:Y861F or FAK:Y925F was reduced compared with FAK:WT (Fig. 9 B), indicating that efficient cross talk from MK cells to endothelial cells requires FAK residues Y861 and Y925.

Because MMP-9 has been implicated in both wound healing and the angiogenic switch (Bergers et al., 2000) and its integrin-dependent expression fits our regulatory pattern of interest (Fig. 8, D and E), we tested the effects of dominant-negative FAK mutants on MMP-9 secretion. We observed reduced secretion of MMP-9 from MK cells infected with either FAK:Y861F or FAK:Y925F compared with FAK:WT (Fig. 9 C). Importantly, treatment with the broad-spectrum MMP inhibitor GM6001 reduced HUVEC migration in response to conditioned medium from MK$\alpha3^+/\alpha9^-$ cells in a dose-dependent manner (Fig. 9 D), implicating an MMP in the paracrine signaling to endothelial cells. Moreover, immunostaining of 5- and 10-d wounds from our panel of epidermis-specific integrin knockout mice revealed a pattern of MMP-9 expression that correlates with higher blood vessel density (compare Fig. 3 with Fig. 10). Collectively, our data support a model wherein α9β1 inhibits α3β1-mediated FAK/Src signaling that induces MMP-9 production by keratinocytes, which may contribute to the suppression of paracrine stimulation of endothelial cells (Fig. 9 E).

Discussion

Integrin α9β1 inhibits keratinocyte to endothelial cell cross talk through cross-suppression of integrin α3β1

Wound healing is a dynamic process that involves communication between multiple cell types within the wound microenvironment that collectively control inflammation, angiogenesis, reepithelialization, scar formation, and tissue remodeling. The epidermis can send paracrine signals to other cellular compartments to help coordinate their functions and ensure proper wound healing (Nowinski et al., 2004; Ghahary and Ghaffari, 2007; Werner et al., 2007). Integrins are likely candidates for mediating such cross talk, as they can translate ECM signals into keratinocyte production of growth factors and extracellular proteases that directly or indirectly stimulate other cells (Mitchell et al., 2009; Margadant and Sonnenberg, 2010; Koivisto et al., 2014; Longmate and DiPersio, 2014). Our previous work identified a novel role for the keratinocyte integrin α3β1 in controlling the production of paracrine-acting factors that stimulate endothelial cells and promote wound angiogenesis (Mitchell et al., 2009). However, the extent to which different integrins function in combination to regulate wound healing has been

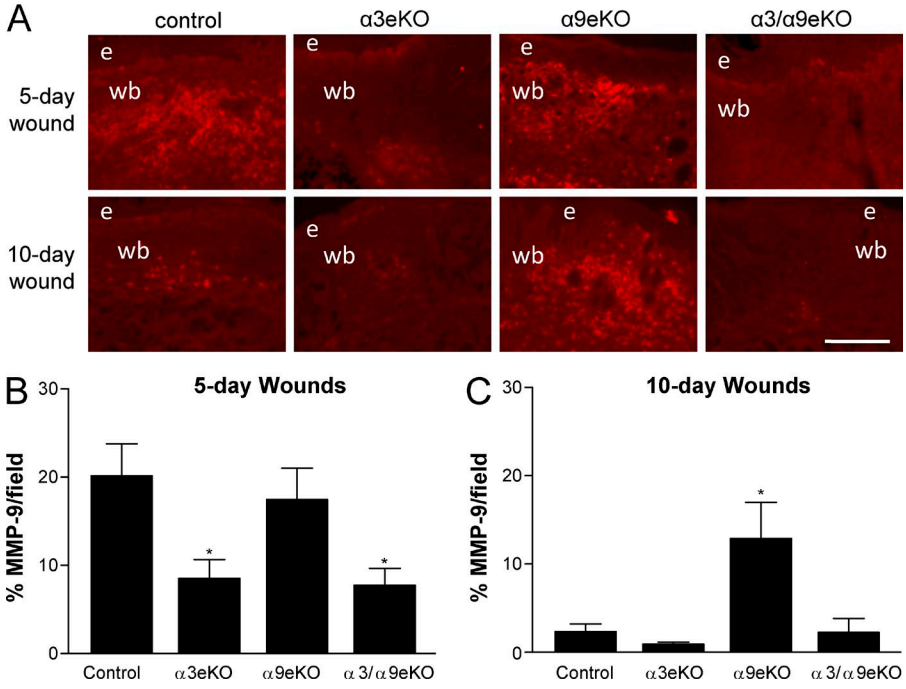

Figure 10. **MMP-9 expression correlates with higher blood vessel density during in vivo wound healing.** (A) MMP-9 immunostaining of cryosections from 5- and 10-d wounds in control, α3eKO, α9eKO, or α3/α9eKO mice. Bar, 100 µm. e, epidermis; wb, wound bed. (B and C) MMP-9 staining was quantified for each genotype as percentages of positive staining per field within 5-d (B) or 10-d (C) wound beds. Means ± SEM are shown. $n \geq 5$ mice per genotype. One-way analyses of variance followed by Newman-Keuls's multiple comparisons test were used. *, $P < 0.05$ compared with nonasterisked groups.

unclear, hindering the development of wound therapies that exploit integrin agonists or antagonists.

Results of the current study identify novel and unexpected combinatorial roles of two epidermal integrins that are upregulated during wound healing, where α9β1 cross-suppresses the proangiogenic functions of α3β1. Indeed, our data in cultured keratinocytes support a model (Fig. 9 E) wherein α3β1 activates a FAK signaling pathway that promotes the production of paracrine-acting factors including MMP-9 that stimulate endothelial cell migration and survival, whereas keratinocyte α9β1 suppresses this pathway at a point downstream of initial FAK autophosphorylation. Importantly, results from our genetic model provide in vivo support for our hypothesis that α9β1 exerts inhibition over α3β1 at later stages of wound healing, thereby governing the temporal progression of epidermal paracrine signals that control vascular density. Indeed, we observed that the healing wounds of mice with epidermal deletion of α9β1, but which express α3β1, displayed normal induction of angiogenesis but delayed vascular normalization, coincident with reduced endothelial apoptosis. Collectively, results from our in vitro and in vivo models indicate that α9β1 acts as a temporally regulated brake on the proangiogenic functions of α3β1. Our findings provide a novel physiological context for cross-regulation between integrins, potentially including mechanisms of trans-dominant inhibition described previously using in vitro models (Díaz-González et al., 1996; Hodivala-Dilke et al., 1998; Calderwood et al., 2004).

We previously showed that α3β1 expression in MK cells promotes FAK activation (i.e., Y397 autophosphorylation) as well as subsequent Src-mediated phosphorylation of FAK Y861 and Y925 (Choma et al., 2007). Our current findings that phosphorylation of FAK Y397 was intact in MKα3$^+$/α9$^+$ cells, whereas that of Y861/Y925 was reduced (Fig. 6), suggest that α9β1 exerts its suppressive effect over α3β1 at the point of Src-mediated FAK phosphorylation (Fig. 9 E). Although the mechanism whereby α9β1 suppresses FAK phosphorylation at the Src substrate sites remains unknown, one intriguing possibility is that α9β1 inhibits or sequesters Src family kinases. We have not ruled out additional points of inhibition, but this regulation was sufficient for α9β1 to cross-suppress α3β1-mediated cross talk to endothelial cells because mutating FAK at either Y861 or Y925 reduced this cross talk (Fig. 9, A and B).

It is likely that α9β1-mediated suppression of paracrine signals from the epidermis occurs in large part through its cross-suppressive effects on α3β1-dependent gene regulation. Indeed, our past studies have shown that α3β1 regulates several MK genes that encode matricellular proteins such as fibulin-2 (Longmate et al., 2014; Missan et al., 2014), extracellular proteases such as MMP-9 (DiPersio et al., 2000; Iyer et al., 2005), and growth factors such as MRP-3 (Mitchell et al., 2009). Moreover, we have linked some of these genes to α3β1-dependent functions in our in vitro and in vivo models, including matrix assembly and paracrine stimulation of angiogenesis (Lamar et al., 2008b; Mitchell et al., 2009; Longmate et al., 2014; Missan et al., 2014). Collectively, our findings support a key role for α3β1 as a regulator of genes that allow keratinocytes to modulate the skin microenvironment, in part through paracrine cross talk to other cells. Importantly, our findings that α9β1 cross-suppresses a subset of α3β1-dependent genes (Fig. 8), including some with known or potential roles in paracrine stimulation of angiogenesis, support our working hypothesis that α9β1 exerts trans-dominant inhibition over α3β1-dependent gene expression that facilitates matrix remodeling and intercellular cross talk.

Integrin cross-suppression provides a mechanism for temporal control over vascular density during wound healing

Our findings establish a novel paradigm in which cross-regulation between two distinct keratinocyte integrins, α9β1 and α3β1, is critical during wound healing to achieve temporally appropriate paracrine signals from the epidermis to endothelial cells that control both the initial angiogenic response and later blood vessel regression. Indeed, although these integrins

can each exert separate influences on keratinocyte function (Singh et al., 2009; Longmate and DiPersio, 2014; Longmate et al., 2014), our current work shows that early proangiogenic functions guided by α3β1 are tempered by α9β1 later in wound healing through a mechanism of cross-suppression. Our model predicts that the ability of α9β1 to modulate α3β1 function is temporally restricted in vivo to promote vascular normalization during the resolution phase. Consistently, suppressive activity of α9β1 over α3β1 was observed only at later stages of wound healing, during the period of vascular regression, at which time α9eKO mice displayed persistently high vascular density and reduced endothelial apoptosis compared with control mice (Figs. 3 and 4). Integrins α3β1 and α9β1 are both up-regulated at the onset of wound healing (Hertle et al., 1991; Singh et al., 2004), suggesting that temporal coordination of their functions may be achieved through binding to ECM ligands that appear at specific stages of wound healing. Indeed, we were able to abrogate the cross-suppressive effects of α9β1 through treatment with the function-blocking antibody Y9A2. Although our data implicate FN as a candidate ligand that could activate the cross-suppressive effect of α9β1 in our wound healing model (Fig. 7), we cannot rule out the importance of other α9β1 ligands.

Activated wound keratinocytes and transformed/tumorigenic keratinocytes share certain properties, including enhanced migration, proliferation, and production of MMPs and proangiogenic factors (Dvorak, 1986; Watt, 2002; Longmate and DiPersio, 2014). Moreover, α3β1 and α9β1 are up-regulated or persist in epidermal tumors (Häkkinen et al., 1999; Janes and Watt, 2006; Longmate and DiPersio, 2014), and α3β1 has paracrine, proangiogenic roles in both wound keratinocytes, and at least some carcinoma cells (Mitchell et al., 2009, 2010). However, an important distinction between wounds and tumors is that the latter do not experience a vascular regression phase, consistent with the long-held notion that a tumor is like a wound that does not heal (Dvorak, 1986; Schäfer and Werner, 2008). Interestingly, epidermal deletion of α9 neither increased α3β1-dependent papilloma growth nor enhanced the vascular density of tumors in the two-step carcinogenesis model, suggesting that the suppressive role of α9β1 that occurs in wound healing, wherein vasculature eventually recedes, is absent during epidermal tumorigenesis, wherein angiogenesis persists. An intriguing possibility is that the suppressive function of α9β1 is lost in skin tumors, thereby promoting persistent wound-like properties and providing a continued α3β1-dependent growth advantage to tumor cells.

Our earlier studies identified MMP-9, a known proangiogenic factor, as an α3β1-dependent gene in MK cells (Iyer et al., 2005; Mitchell et al., 2009). In this study, we showed that α3β1-dependent MMP-9 expression was inhibited by α9β1 (Fig. 8, D and E), possibly implicating this MMP in a temporally controlled, integrin-dependent "switch" that governs vascular density in wounds. Indeed, MMP-9 can release ECM-bound vascular endothelial growth factor to stimulate endothelial cells and promote angiogenesis (Bergers et al., 2000; McCawley and Matrisian, 2001), and reduced vascular endothelial growth factor can lead to endothelial cell apoptosis and promote blood vessel regression (Verheul and Pinedo, 2007). Future studies will investigate whether regulation of epidermally derived MMP-9 controls α3β1-dependent wound angiogenesis and α9β1-dependent vascular regression.

Combinatorial functions of integrins: Implications for novel wound therapies

Although integrin-targeting strategies have reached the clinic for several disorders (Goodman and Picard, 2012), such therapies for wound healing have lagged behind because of our incomplete understanding of how keratinocyte integrins regulate this process. In particular, because many epidermal functions are governed by multiple integrins (Watt, 2002; Margadant et al., 2010), progress toward therapies that target integrins requires further investigation into the combined roles of different integrins in wound keratinocytes as well as how distinct integrin–ECM interactions are spatially and temporally coordinated during wound healing. Our current study implicates epidermal integrins α9β1 and α3β1 as potential therapeutic targets for the treatment of wound pathologies, and it provides a foundation for the development of novel strategies that target these integrins at appropriate stages.

Although the importance of the epidermis in wound reepithelialization and restoration of barrier function is well established, it has become clear that epidermal keratinocytes also produce growth factors, cytokines, and ECM proteases that can diffuse to stromal wound cells such as fibroblasts/myofibroblasts, inflammatory cells, and endothelial cells (Singer and Clark, 1999; Santoro and Gaudino, 2005). Moreover, dysfunctional paracrine cross talk from the epidermis to other wound cells may contribute to wound-healing pathologies (Koivisto et al., 2014). For example, stunted wound angiogenesis is a critical feature of chronic, insufficient wound healing (e.g., diabetic ulcers), whereas persistently activated keratinocytes are prominent in overexuberant healing (e.g., hypertrophic scars; Machesney et al., 1998; Kota et al., 2012). Given the role that we have identified for integrin α3β1 in the paracrine stimulation of wound angiogenesis and the inhibition of this function by the integrin α9β1, it is interesting to speculate that altered expression or function of these integrins leads to defective intercellular communication in some pathological wounds. Future studies will address this possibility in human clinical specimens.

In summary, our current findings provide a rationale for novel integrin-targeting therapeutics to modulate keratinocyte function and improve wound outcome. This approach includes the concept of using α9β1-targeting antagonists or agonists to promote or abrogate, as appropriate, α3β1-dependent functions of the wound epidermis. We speculate that promoting α3β1 function by inhibiting α9β1 (or inhibiting α3β1 function by activating α9β1) may have a multicombinatorial effect because our data show that these two integrins coordinately regulate several keratinocyte genes representing a spectrum of both soluble and adhesive factors with potential roles in wound healing.

Materials and methods

Derivation of MK cell variants

Keratinocyte growth medium consisted of Eagle's minimum essential medium (BioWhittaker) supplemented with 4% fetal bovine serum (BioWhittaker) from which Ca^{2+} had been chelated, 0.05 mM $CaCl_2$, 0.04 µg/ml hydrocortisone, 5 µg/ml insulin, 2×10^{-9} M T3, 10 U/ml interferon-γ (Sigma-Aldrich), 10 ng/ml epidermal growth factor, 100 U/ml penicillin, 100 µg/ml streptomycin, and L-glutamine (Invitrogen). Keratinocytes were maintained at 33°C and 8% CO_2 on tissue culture

dishes coated with 30 µg/ml denatured rat tail collagen (BD). The parental MK line (MKα3^{-}/α9^{-}) was derived from the epidermis of a neonatal α3-null mouse as described previously (DiPersio et al., 2000); keratinocytes lose integrin α9 expression upon subculture (Singh et al., 2009). First, human α3 was stably transfected into MKα3^{-}/α9^{-} cells to generate MKα3^{+}/α9^{-} cells. Next, we used a retroviral approach to introduce human α9 into each of the latter variants to generate MKα3^{-}/α9^{+} cells and MKα3^{+}/α9^{+} cells. Human α9 expression was linked to GFP expression through an IRES (MSCV-α9-IRES-GFP). FACS for GFP-positive cells was performed to enrich for the desired populations, and similar surface expression of α3β1 and/or α9β1 among the MK variants was confirmed by flow cytometry using mAbs specific for the human α3 (P1B5) or α9 (Y9A2; EMD Millipore) subunits, respectively. Surface expression of mouse integrin α2 (CD49b; EMD Millipore), α5 (5H10-27; BD), and α6 (GoH3; EMD Millipore) was similarly assessed.

In vitro scrape wound migration assays

Scrape wound assays were performed essentially as described previously (Choma et al., 2004). In brief, MK cells were grown to confluence on LN-332–rich ECM prepared from the human SCC cell line SCC-25 as described previously (Xia et al., 1996). Cultures were serum starved overnight, scrape wounded with the narrow end of a 200-µl pipette tip, and then rinsed several times with PBS to dislodge remaining cells. Phase images of live cultures were collected 0, 8, and 24 h after scraping on an upright microscope (Eclipse 80*i*; Nikon; 10× objective) using a Spot camera (Diagnostic Instruments).

Transwell migration of HUVECs

HUVECs from pooled donors were purchased from VEC Technologies and grown in complete EGM-2 medium (Lonza) at 37°C and 5% CO_2 on tissue culture dishes coated with 0.2% gelatin. Transwell migration assays were performed as described previously (Mitchell et al., 2009). In brief, transwell tissue culture inserts with 8-µm pores (Costar) were coated with 0.2% gelatin overnight. HUVECs were serum starved for 24 h, trypsinized, and seeded onto top surfaces of transwells at 5×10^4 cells per insert. Lower chambers contained serum-free EBM-2 medium (Lonza) that had been conditioned by the indicated MK cell variants in a 7:3 ratio with complete EGM-2 medium (Mitchell et al., 2009) with or without the MMP inhibitor GM 6001 (Santa Cruz Biotechnology, Inc.), as indicated. After 4 h at 37°C, migrated cells were fixed, permeabilized, and stained with DAPI (Thermo Fisher Scientific). Migrated HUVECs were visualized in room temperature PBS using an inverted microscope (IX70; Olympus; 4× objective), and images were collected using a digital camera (SensiCam; Cooke). The total stained area was quantified using ImageJ software (National Institutes of Health).

Analysis of HUVEC apoptosis in vitro

HUVECs were serum starved for 24 h and then treated for 6 h with serum-free EBM-2 medium that had been conditioned overnight by the indicated MK cell variant. Apoptosis was assessed in HUVECs either using the EnzChek Caspase 3 Assay kit (Molecular Probes) to measure caspase 3 proteolytic activity or by immunostaining with anti–cleaved caspase 3. For the former, data were collected on a Synergy 2 microplate reader using Gen5 software (BioTek). For immunostaining, treated HUVECs were fixed in 3.7% formaldehyde, permeabilized in 0.1% Triton X-100, blocked in 10% heat-inactivated goat serum/5% milk/PBS for 1 h, and then stained with anti–cleaved caspase 3 (Cell Signaling Technology) followed by Alexa Fluor 594 goat anti–rabbit IgG (Molecular Probes) and DAPI (Thermo Fisher Scientific). Cells were imaged in ProLong gold antifade mounting medium (Molecular Probes) at room temperature on an Eclipse 80*i* upright microscope (20× objective) using a Spot camera.

Conditional integrin knockout mice

Epidermis-specific α3eKO mice and epidermis-specific α9eKO mice are homozygous for a floxed α3 allele (Itga3$^{flx/flx}$) or α9 allele (Itga9$^{flx/flx}$), respectively, and express a Cre recombinase transgene under the control of the epidermis-specific keratin 14 promoter (K14-Cre) as previously described (Mitchell et al., 2009; Singh et al., 2009). The double-knockout (α3/α9eKO) mice were generated by crossing α3eKO mice with α9eKO mice. PCR genotyping of α3eKO mice (i.e., genotype K14-Cre:Itga3$^{flx/flx}$), α9eKO mice (i.e., genotype K14-Cre:Itga9$^{flx/flx}$), α3/α9eKO mice (i.e., genotype K14-Cre:Itga3$^{flx/flx}$:Itga9$^{flx/flx}$), or control littermates that lack the K14-Cre transgene was performed as described previously (Mitchell et al., 2009; Singh et al., 2009). Absence of α3β1 and/or α9β1 from the epidermis of α3eKO or α9eKO mice was confirmed by immunostaining for the α3 and α9 integrin subunits (Mitchell et al., 2009; Singh et al., 2009). All mouse studies were approved by the Institutional Animal Care and Use Committee at Albany Medical College.

In vivo wounding and acquisition of tissue

Adult mice (6–10 wk of age) were anesthetized and shaved, and four full-thickness wounds were made on the back of each mouse using a sterile 4-mm biopsy punch as described previously (Mitchell et al., 2009). After 3, 4, 5, or 10 d, mice were euthanized by CO_2 narcosis, and wounds were surgically excised along with a sample of distal unwounded skin and were either frozen in optimum cutting temperature compound (Electron Microscopy Sciences) or fixed in 4% paraformaldehyde, embedded in paraffin, sectioned (5 µm), and stained with hematoxylin and eosin.

Two-step skin carcinogenesis

The backs of 7-wk-old mice were shaved and treated with a single dose of DMBA (30 µg in 200 µl acetone) followed by twice-weekly applications of TPA (12.34 µg in 200 µl acetone) for 20 wk (Sachs et al., 2012). Papillomas of >1-mm diameter were counted and measured every other week starting at 18 wk of age (treatment week 11). Tumor length (l) and width (w) were measured using a Vernier caliper, and the tumor volume was calculated using the following formula: tumor volume = $(w^2 \times l)/2$. Statistical analyses were performed on data collected after 21 wk of treatment. At that time, papillomas were excised and frozen in optimum cutting temperature compound.

Immunohistology of tissue sections

10-µm frozen tissue sections were rehydrated in 0.2% Tween 20/PBS for 10 min, fixed in 3.7% formaldehyde, permeabilized in 0.5% Triton X-100, blocked in 10% heat-inactivated goat serum/5% milk/PBS for 1 h, and then stained with anti–cleaved caspase 3, anti-CD31 (BD), anti–LN-332 (Abcam), anti-FN (Sigma-Aldrich), anti–MMP-9 (Sigma-Aldrich), or anti–keratin 14 (Covance). Immunostaining was also performed using antibodies against integrin α2 (CD49b; EMD Millipore), α5 (5H10-27; BD), and α6 (GoH3; EMD Millipore). Secondary antibodies were Alexa Fluor 488 goat anti–rat IgG, Alexa Fluor 488 goat anti–hamster IgG, Alexa Fluor 594 goat anti–mouse IgG, or Alexa Fluor 594 goat anti–rabbit IgG (Molecular Probes), as appropriate. Images were collected on an Eclipse 80*i* upright microscope using a Spot camera. For assessment of wound immunostaining, the field within the wound bed below the reepithelialized epidermis was imaged. For assessment of vessel density within papillomas, nonnecrotic tumor regions were imaged. CD31 and MMP-9 staining was quantified using ImageJ software.

Western blotting

Cells were adhered to collagen-coated dishes in keratinocyte growth medium as described in the Derivation of MK cell variants section,

under which conditions they deposit endogenous LN-332 (Choma et al., 2004). Total lysates were prepared in cell lysis buffer (Cell Signaling Technology) containing protease and phosphatase inhibitors, and protein concentrations were determined using the BCA Protein Assay kit (Thermo Fisher Scientific). Equal protein was resolved by nonreducing 10% SDS/PAGE, transferred to nitrocellulose, and probed with the antibodies anti-FAK pY397 (Cell Signaling Technology), anti-FAK pY861 (Abcam), anti-FAK pY925 (Cell Signaling Technology), or total FAK (BD). Chemiluminescence was performed using the SuperSignal kit (Thermo Fisher Scientific) and then was quantified using a ChemiDoc MP imaging system with Image Lab software (Bio-Rad Laboratories).

Assessment of α9β1-mediated cell adhesion

Cells were suspended and preincubated with 10 µg/ml Y9A2 or control mouse IgG (EMD Millipore) for 30 min on ice. Adhesion assays were performed by plating preincubated cells onto wells coated with 1 µM EIIIA FN (Shinde et al., 2008). Cells were allowed to adhere for 2 h at 33°C and then were stained with crystal violet. Crystal violet was liberated and quantitation was performed by reading the absorbance at 580 nM using a Synergy 2 microplate reader with Gen5 software (BioTek). For signaling experiments, cells were preincubated with Y9A2 or mouse IgG as described, adhered to collagen-coated wells, and then were assessed by immunoblotting as described in the previous section.

Adenoviral infection of MK cells

Human FAK constructs were provided by J. Zhao (University of Central Florida, Orlando, FL). Adenoviruses were constructed using the AdEasy system as previously described (Bryant et al., 2006). Cells were seeded onto collagen-coated 6-well dishes and infected for 24 h. Infection conditions were optimized to achieve GFP-FAK:wt, GFP-FAK:Y861F, or GFP-FAK:Y925F expression levels that were comparably higher than levels of endogenous FAK, as we described previously (Choma et al., 2007). Adenoviral infection efficiency was >90% for all constructs, as assessed by visualizing GFP-positive cells.

Gene microarrays and quantitative PCR

Microarrays were performed to compare gene expression in MK cells expressing α3β1 alone (MKα3$^+$/α9$^-$), α9β1 alone (MKα3$^-$/α9$^+$), or both integrins (MKα3$^+$/α9$^+$) to baseline expression in MKα3$^-$/α9$^-$. In brief, mRNA was purified from MK variants cultured for 1 d on collagen, onto which they deposited LN-332 and cFN, based on our published studies of α3β1-dependent induction of MMP-9 or MRP-3 genes (DiPersio et al., 2000; Mitchell et al., 2009). mRNA was purified using the RNeasy Plus kit (QIAGEN), and quality was confirmed on a Bioanalyzer (Agilent Technologies). Gene expression was measured using whole-genome arrays (Mouse Gene ST 1.0; Affymetrix; full coding sequences for 28,853 genes), analyzed with Affymetrix software, imported into GeneSpring (Agilent Technologies), normalized, and subjected to an analysis of variance ($P < 0.05$) with a multiple correction factor (Benjamin-Hochberg or Bonferroni) to remove false positives, as described previously (Missan et al., 2014). Data were subject to hierarchical clustering, and pairwise comparisons were made to identify gene clusters that are regulated either by each integrin alone or both integrins together relative to baseline expression in MKα3$^-$/α9$^-$ cells. Transcripts that were detected at levels significantly above or below our threshold were displayed in heat maps for each MK variant. The complete gene list was submitted to the Gene Expression Omnibus (series accession no. GSE73826).

Individual quantitative PCR for MMP-9 was performed using iQ SYBR green Supermix on a MyiQ PCR machine (Bio-Rad Laboratories). cDNA was generated using iScript Reverse Transcription Supermix (Bio-Rad Laboratories). Conditions for MMP-9 were forward primer, 5′-CAGCTGGCAGAGGCATACTTG-3′; reverse primer, 5′-GCTTCTCTCCCATCATCTGGG-3′; 94°C for 3 min for one cycle, followed by 94°C for 30 s, 54°C for 30 s, and 72°C for 30 s, for 40 cycles (Lamar et al., 2008a). Conditions for β-actin were forward primer, 5′-AGGGAAATCGTGCGTGACAT-3′; reverse primer, 5′-CATCTG CTGGAAGGTGGACA-3′; 95°C for 10 min for one cycle, followed by 94°C for 1 min, 58°C for 90 s, and 72°C for 90 s, for 35 cycles (Missan et al., 2014). Relative mRNA levels were calculated using the following formula: (2^ − [Ct MMP-9 gene − Ct β-actin gene]) × 100 (Missan et al., 2014).

Gelatin zymography

4×10^5 MK cells were plated onto 6-well dishes in full MK medium overnight and then were washed and cultured in 2 ml of serum-free medium without antibiotics or interferon-γ for 24 h. Culture medium was collected and incubated with gelatin-agarose beads overnight at 4°C. Beads were recovered by centrifugation, and bound MMPs were eluted in sample buffer (2.25% SDS, 9% glycerol, 45 mM Tris-HCl, pH 6.8, and bromophenol blue) and resolved by nonreducing SDS-PAGE on gelatin-impregnated 10% polyacrylamide gels (Iyer et al., 2005). After electrophoresis, gels were soaked in 2.5% Triton X-100, washed with water, and then incubated overnight at 37°C in MMP activation buffer (50 mM Tris, pH 8.0, and 5 mM $CaCl_2$). Gels were stained with Coomassie blue and then destained in 10% methanol and 5% acetic acid, and gelatinase activity was revealed as clear bands on a blue background (DiPersio et al., 2000).

Online supplemental material

Fig. S1 confirms appropriate expression of α3β1 and α9β1 in MK cell variants. Fig. S2 shows that α9β1 inhibits α3β1-dependent scratch wound closure in vitro but not wound reepithelialization in vivo. Fig. S3 confirms deletion of α3 or α9 integrin subunits in the epidermis of the respective epidermal knockout mice. Fig. S4 demonstrates that expression levels of other β1 integrins are similar in keratinocytes or epidermis with manipulated expression of α3β1, α9β1, or both. Fig. S5 shows that the paxillin-binding site of the α9 cytoplasmic tail is not required for α9β1 to suppress the α3β1-dependent induction of HUVEC migration by MK cells.

Acknowledgments

We thank Christina Nickerson (Albany Medical Center Histology Core) for assistance with tissue sectioning and Lei Wu for generating the α9 paxillin-binding mutant. Additional technical assistance was provided by Drs. Patrick Bryant and Tessa Simone as well as Derek Power, Courtney Betts, Alexander Granick, and Savitha Sambandamoorthy. We thank Dr. Peter Vincent for assistance with statistical analyses. Finally, we thank Drs. Susan LaFlamme and Sita Subbaram for helpful discussion and critical review of the manuscript.

This research was supported by National Institutes of Health grants from the National Institute of Arthritis and Musculoskeletal and Skin Diseases to L. Van De Water and C.M. DiPersio (R01AR063778) and from the National Cancer Institute to C.M. DiPersio (R01CA-129637) as well as by a National Institutes of Health predoctoral fellowship from the National Cancer Institute to W.M. Longmate (F31CA174198).

The authors declare no competing financial interests.

Author contributions: W.M. Longmate and S.P. Lyons designed and performed experiments and analyzed data. S.V. Chittur performed gene microarrays and associated analyses. K.M. Pumiglia provided key reagents and contributed expert advice to the design

and interpretation of experiments. C.M. DiPersio and L. Van De Water conceived the project. W.M. Longmate, C.M. DiPersio, and L. Van De Water wrote the manuscript with contributions from all authors.

Submitted: 12 October 2015
Revised: 10 February 2017
Accepted: 14 March 2017

References

Bergers, G., R. Brekken, G. McMahon, T.H. Vu, T. Itoh, K. Tamaki, K. Tanzawa, P. Thorpe, S. Itohara, Z. Werb, and D. Hanahan. 2000. Matrix metalloproteinase-9 triggers the angiogenic switch during carcinogenesis. *Nat. Cell Biol.* 2:737–744. http://dx.doi.org/10.1038/35036374

Bryant, P., Q. Zheng, and K. Pumiglia. 2006. Focal adhesion kinase controls cellular levels of p27/Kip1 and p21/Cip1 through Skp2-dependent and -independent mechanisms. *Mol. Cell. Biol.* 26:4201–4213. http://dx.doi.org/10.1128/MCB.01612-05

Calderwood, D.A., V. Tai, G. Di Paolo, P. De Camilli, and M.H. Ginsberg. 2004. Competition for talin results in trans-dominant inhibition of integrin activation. *J. Biol. Chem.* 279:28889–28895. http://dx.doi.org/10.1074/jbc.M402161200

Cary, L.A., and J.L. Guan. 1999. Focal adhesion kinase in integrin-mediated signaling. *Front. Biosci.* 4:D102–D113. http://dx.doi.org/10.2741/Cary

Choma, D.P., K. Pumiglia, and C.M. DiPersio. 2004. Integrin α3β1 directs the stabilization of a polarized lamellipodium in epithelial cells through activation of Rac1. *J. Cell Sci.* 117:3947–3959. http://dx.doi.org/10.1242/jcs.01251

Choma, D.P., V. Milano, K.M. Pumiglia, and C.M. DiPersio. 2007. Integrin α3β1-dependent activation of FAK/Src regulates Rac1-mediated keratinocyte polarization on laminin-5. *J. Invest. Dermatol.* 127:31–40. http://dx.doi.org/10.1038/sj.jid.5700505

Díaz-González, F., J. Forsyth, B. Steiner, and M.H. Ginsberg. 1996. Trans-dominant inhibition of integrin function. *Mol. Biol. Cell.* 7:1939–1951. http://dx.doi.org/10.1091/mbc.7.12.1939

DiPersio, C.M., M. Shao, L. Di Costanzo, J.A. Kreidberg, and R.O. Hynes. 2000. Mouse keratinocytes immortalized with large T antigen acquire alpha-3beta1 integrin-dependent secretion of MMP-9/gelatinase B. *J. Cell Sci.* 113:2909–2921.

Dvorak, H.F. 1986. Tumors: Wounds that do not heal. *N. Engl. J. Med.* 315:1650–1659. http://dx.doi.org/10.1056/NEJM198612253152606

Ghahary, A., and A. Ghaffari. 2007. Role of keratinocyte–fibroblast cross-talk in development of hypertrophic scar. *Wound Repair Regen.* 15:S46–S53. http://dx.doi.org/10.1111/j.1524-475X.2007.00225.x

Giancotti, F.G., and E. Ruoslahti. 1999. Integrin signaling. *Science.* 285:1028–1033. http://dx.doi.org/10.1126/science.285.5430.1028

Gonzalez, A.M., R. Bhattacharya, G.W. deHart, and J.C. Jones. 2010. Transdominant regulation of integrin function: mechanisms of crosstalk. *Cell. Signal.* 22:578–583. http://dx.doi.org/10.1016/j.cellsig.2009.10.009

Goodman, S.L., and M. Picard. 2012. Integrins as therapeutic targets. *Trends Pharmacol. Sci.* 33:405–412. http://dx.doi.org/10.1016/j.tips.2012.04.002

Grose, R., C. Hutter, W. Bloch, I. Thorey, F.M. Watt, R. Fässler, C. Brakebusch, and S. Werner. 2002. A crucial role of β1 integrins for keratinocyte migration in vitro and during cutaneous wound repair. *Development.* 129:2303–2315.

Häkkinen, L., T. Kainulainen, T. Salo, R. Grenman, and H. Larjava. 1999. Expression of integrin α9 subunit and tenascin in oral leukoplakia, lichen planus, and squamous cell carcinoma. *Oral Dis.* 5:210–217. http://dx.doi.org/10.1111/j.1601-0825.1999.tb00303.x

Hertle, M.D., J.C. Adams, and F.M. Watt. 1991. Integrin expression during human epidermal development in vivo and in vitro. *Development.* 112:193–206.

Hodivala-Dilke, K.M., C.M. DiPersio, J.A. Kreidberg, and R.O. Hynes. 1998. Novel roles for α3β1 integrin as a regulator of cytoskeletal assembly and as a trans-dominant inhibitor of integrin receptor function in mouse keratinocytes. *J. Cell Biol.* 142:1357–1369. http://dx.doi.org/10.1083/jcb.142.5.1357

Høye, A.M., J.R. Couchman, U.M. Wewer, K. Fukami, and A. Yoneda. 2012. The newcomer in the integrin family: integrin α9 in biology and cancer. *Adv. Biol. Regul.* 52:326–339. http://dx.doi.org/10.1016/j.jbior.2012.03.004

Hynes, R.O. 2002. Integrins: Bidirectional, allosteric signaling machines. *Cell.* 110:673–687. http://dx.doi.org/10.1016/S0092-8674(02)00971-6

Iyer, V., K. Pumiglia, and C.M. DiPersio. 2005. α3β1 integrin regulates MMP-9 mRNA stability in immortalized keratinocytes: a novel mechanism of integrin-mediated MMP gene expression. *J. Cell Sci.* 118:1185–1195. http://dx.doi.org/10.1242/jcs.01708

Janes, S.M., and F.M. Watt. 2006. New roles for integrins in squamous-cell carcinoma. *Nat. Rev. Cancer.* 6:175–183. http://dx.doi.org/10.1038/nrc1817

Koivisto, L., J. Heino, L. Häkkinen, and H. Larjava. 2014. Integrins in wound healing. *Adv. Wound Care (New Rochelle).* 3:762–783. http://dx.doi.org/10.1089/wound.2013.0436

Kota, S.K., L.K. Meher, S. Jammula, S.K. Kota, S.V. Krishna, and K.D. Modi. 2012. Aberrant angiogenesis: The gateway to diabetic complications. *Indian J. Endocrinol. Metab.* 16:918–930. http://dx.doi.org/10.4103/2230-8210.102992

Lamar, J.M., V. Iyer, and C.M. DiPersio. 2008a. Integrin α3β1 potentiates TGFβ-mediated induction of MMP-9 in immortalized keratinocytes. *J. Invest. Dermatol.* 128:575–586. http://dx.doi.org/10.1038/sj.jid.5701042

Lamar, J.M., K.M. Pumiglia, and C.M. DiPersio. 2008b. An immortalization-dependent switch in integrin function up-regulates MMP-9 to enhance tumor cell invasion. *Cancer Res.* 68:7371–7379. http://dx.doi.org/10.1158/0008-5472.CAN-08-1080

Litjens, S.H., J.M. de Pereda, and A. Sonnenberg. 2006. Current insights into the formation and breakdown of hemidesmosomes. *Trends Cell Biol.* 16:376–383. http://dx.doi.org/10.1016/j.tcb.2006.05.004

Liu, S., M. Slepak, and M.H. Ginsberg. 2001. Binding of paxillin to the α_9 integrin cytoplasmic domain inhibits cell spreading. *J. Biol. Chem.* 276:37086–37092. http://dx.doi.org/10.1074/jbc.M105114200

Longmate, W.M., and C.M. DiPersio. 2014. Integrin regulation of epidermal functions in wounds. *Adv. Wound Care (New Rochelle).* 3:229–246. http://dx.doi.org/10.1089/wound.2013.0516

Longmate, W.M., R. Monichan, M.L. Chu, T. Tsuda, M.G. Mahoney, and C.M. DiPersio. 2014. Reduced fibulin-2 contributes to loss of basement membrane integrity and skin blistering in mice lacking integrin α3β1 in the epidermis. *J. Invest. Dermatol.* 134:1609–1617. http://dx.doi.org/10.1038/jid.2014.10

Machesney, M., N. Tidman, A. Waseem, L. Kirby, and I. Leigh. 1998. Activated keratinocytes in the epidermis of hypertrophic scars. *Am. J. Pathol.* 152:1133–1141.

Manohar, A., S.G. Shome, J. Lamar, L. Stirling, V. Iyer, K. Pumiglia, and C.M. DiPersio. 2004. α3β1 integrin promotes keratinocyte cell survival through activation of a MEK/ERK signaling pathway. *J. Cell Sci.* 117:4043–4054. http://dx.doi.org/10.1242/jcs.01277

Margadant, C., and A. Sonnenberg. 2010. Integrin–TGF-β crosstalk in fibrosis, cancer and wound healing. *EMBO Rep.* 11:97–105. http://dx.doi.org/10.1038/embor.2009.276

Margadant, C., K. Raymond, M. Kreft, N. Sachs, H. Janssen, and A. Sonnenberg. 2009. Integrin α3β1 inhibits directional migration and wound re-epithelialization in the skin. *J. Cell Sci.* 122:278–288. http://dx.doi.org/10.1242/jcs.029108

Margadant, C., R.A. Charafeddine, and A. Sonnenberg. 2010. Unique and redundant functions of integrins in the epidermis. *FASEB J.* 24:4133–4152. http://dx.doi.org/10.1096/fj.09-151449

McCawley, L.J., and L.M. Matrisian. 2001. Matrix metalloproteinases: they're not just for matrix anymore! *Curr. Opin. Cell Biol.* 13:534–540. http://dx.doi.org/10.1016/S0955-0674(00)00248-9

Missan, D.S., S.V. Chittur, and C.M. DiPersio. 2014. Regulation of fibulin-2 gene expression by integrin α3β1 contributes to the invasive phenotype of transformed keratinocytes. *J. Invest. Dermatol.* 134:2418–2427. http://dx.doi.org/10.1038/jid.2014.166

Missan, D.S., K. Mitchell, S. Subbaram, and C.M. DiPersio. 2015. Integrin α3β1 signaling through MEK/ERK determines alternative polyadenylation of the MMP-9 mRNA transcript in immortalized mouse keratinocytes. *PLoS One.* 10:e0119539. http://dx.doi.org/10.1371/journal.pone.0119539

Mitchell, K., C. Szekeres, V. Milano, K.B. Svenson, M. Nilsen-Hamilton, J.A. Kreidberg, and C.M. DiPersio. 2009. α3β1 integrin in epidermis promotes wound angiogenesis and keratinocyte-to-endothelial-cell crosstalk through the induction of MRP3. *J. Cell Sci.* 122:1778–1787. http://dx.doi.org/10.1242/jcs.040956

Mitchell, K., K.B. Svenson, W.M. Longmate, K. Gkirtzimanaki, R. Sadej, X. Wang, J. Zhao, A.G. Eliopoulos, F. Berditchevski, and C.M. DiPersio. 2010. Suppression of integrin α3β1 in breast cancer cells reduces *cyclooxygenase-2* gene expression and inhibits tumorigenesis, invasion, and cross-talk to endothelial cells. *Cancer Res.* 70:6359–6367. http://dx.doi.org/10.1158/0008-5472.CAN-09-4283

Mitra, S.K., and D.D. Schlaepfer. 2006. Integrin-regulated FAK-Src signaling in normal and cancer cells. *Curr. Opin. Cell Biol.* 18:516–523. http://dx.doi.org/10.1016/j.ceb.2006.08.011

Nguyen, B.P., M.C. Ryan, S.G. Gil, and W.G. Carter. 2000. Deposition of laminin 5 in epidermal wounds regulates integrin signaling and adhesion. *Curr. Opin. Cell Biol.* 12:554–562. http://dx.doi.org/10.1016/S0955-0674(00)00131-9

Nishiya, N., W.B. Kiosses, J. Han, and M.H. Ginsberg. 2005. An α_4 integrin–paxillin–Arf-GAP complex restricts Rac activation to the leading edge of migrating cells. *Nat. Cell Biol.* 7:343–352. http://dx.doi.org/10.1038/ncb1234

Nowinski, D., A.S. Lysheden, H. Gardner, K. Rubin, B. Gerdin, and M. Ivarsson. 2004. Analysis of gene expression in fibroblasts in response to keratinocyte-derived factors in vitro: Potential implications for the wound healing process. *J. Invest. Dermatol.* 122:216–221. http://dx.doi.org/10.1046/j.0022-202X.2003.22112.x

Ridley, A.J., M.A. Schwartz, K. Burridge, R.A. Firtel, M.H. Ginsberg, G. Borisy, J.T. Parsons, and A.R. Horwitz. 2003. Cell migration: integrating signals from front to back. *Science.* 302:1704–1709. http://dx.doi.org/10.1126/science.1092053

Sachs, N., P. Secades, L. van Hulst, M. Kreft, J.Y. Song, and A. Sonnenberg. 2012. Loss of integrin α3 prevents skin tumor formation by promoting epidermal turnover and depletion of slow-cycling cells. *Proc. Natl. Acad. Sci. USA.* 109:21468–21473. http://dx.doi.org/10.1073/pnas.1204614110

Santoro, M.M., and G. Gaudino. 2005. Cellular and molecular facets of keratinocyte reepithelization during wound healing. *Exp. Cell Res.* 304:274–286. http://dx.doi.org/10.1016/j.yexcr.2004.10.033

Schäfer, M., and S. Werner. 2008. Cancer as an overhealing wound: an old hypothesis revisited. *Nat. Rev. Mol. Cell Biol.* 9:628–638. http://dx.doi.org/10.1038/nrm2455

Schlaepfer, D.D., and S.K. Mitra. 2004. Multiple connections link FAK to cell motility and invasion. *Curr. Opin. Genet. Dev.* 14:92–101. http://dx.doi.org/10.1016/j.gde.2003.12.002

Shinde, A.V., C. Bystroff, C. Wang, M.G. Vogelezang, P.A. Vincent, R.O. Hynes, and L. Van De Water. 2008. Identification of the peptide sequences within the EIIIA (EDA) segment of fibronectin that mediate integrin α9β1-dependent cellular activities. *J. Biol. Chem.* 283:2858–2870. http://dx.doi.org/10.1074/jbc.M708306200

Sieg, D.J., C.R. Hauck, D. Ilic, C.K. Klingbeil, E. Schaefer, C.H. Damsky, and D.D. Schlaepfer. 2000. FAK integrates growth-factor and integrin signals to promote cell migration. *Nat. Cell Biol.* 2:249–256. http://dx.doi.org/10.1038/35010517

Singer, A.J., and R.A. Clark. 1999. Cutaneous wound healing. *N. Engl. J. Med.* 341:738–746. http://dx.doi.org/10.1056/NEJM199909023411006

Singh, P., C.L. Reimer, J.H. Peters, M.A. Stepp, R.O. Hynes, and L. Van De Water. 2004. The spatial and temporal expression patterns of integrin α9β1 and one of its ligands, the EIIIA segment of fibronectin, in cutaneous wound healing. *J. Invest. Dermatol.* 123:1176–1181. http://dx.doi.org/10.1111/j.0022-202X.2004.23485.x

Singh, P., C. Chen, S. Pal-Ghosh, M.A. Stepp, D. Sheppard, and L. Van De Water. 2009. Loss of integrin α9β1 results in defects in proliferation, causing poor re-epithelialization during cutaneous wound healing. *J. Invest. Dermatol.* 129:217–228. http://dx.doi.org/10.1038/jid.2008.201

Uotila, L.M., F. Jahan, L. Soto Hinojosa, E. Melandri, M. Grönholm, and C.G. Gahmberg. 2014. Specific phosphorylations transmit signals from leukocyte β2 to β1 integrins and regulate adhesion. *J. Biol. Chem.* 289:32230–32242. http://dx.doi.org/10.1074/jbc.M114.588111

Verheul, H.M., and H.M. Pinedo. 2007. Possible molecular mechanisms involved in the toxicity of angiogenesis inhibition. *Nat. Rev. Cancer.* 7:475–485. http://dx.doi.org/10.1038/nrc2152

Watt, F.M. 2002. Role of integrins in regulating epidermal adhesion, growth and differentiation. *EMBO J.* 21:3919–3926. http://dx.doi.org/10.1093/emboj/cdf399

Werner, S., T. Krieg, and H. Smola. 2007. Keratinocyte-fibroblast interactions in wound healing. *J. Invest. Dermatol.* 127:998–1008. http://dx.doi.org/10.1038/sj.jid.5700786

Wietecha, M.S., W.L. Cerny, and L.A. DiPietro. 2013. Mechanisms of vessel regression: toward an understanding of the resolution of angiogenesis. *Curr. Top. Microbiol. Immunol.* 367:3–32.

Xia, Y., S.G. Gil, and W.G. Carter. 1996. Anchorage mediated by integrin alpha6beta4 to laminin 5 (epiligrin) regulates tyrosine phosphorylation of a membrane-associated 80-kD protein. *J. Cell Biol.* 132:727–740. http://dx.doi.org/10.1083/jcb.132.4.727

Young, B.A., Y. Taooka, S. Liu, K.J. Askins, Y. Yokosaki, S.M. Thomas, and D. Sheppard. 2001. The cytoplasmic domain of the integrin α9 subunit requires the adaptor protein paxillin to inhibit cell spreading but promotes cell migration in a paxillin-independent manner. *Mol. Biol. Cell.* 12:3214–3225. http://dx.doi.org/10.1091/mbc.12.10.3214

Zweers, M.C., J.M. Davidson, A. Pozzi, R. Hallinger, K. Janz, F. Quondamatteo, B. Leutgeb, T. Krieg, and B. Eckes. 2007. Integrin α2β1 is required for regulation of murine wound angiogenesis but is dispensable for reepithelialization. *J. Invest. Dermatol.* 127:467–478. http://dx.doi.org/10.1038/sj.jid.5700546